NIST-GCR-94-653

AN INVESTIGATION OF OIL AND GAS WELL FIRES AND FLARES

P. Dutta, Y. R. Sivathanu, and J. P. Gore

United States Department of Commerce
Technology Administration
National Institute of Standards and Technology

NIST-GCR-94-653

AN INVESTIGATION OF OIL AND GAS WELL FIRES AND FLARES

P. Dutta, Y. R. Sivathanu, and J. P. Gore
School of Mechanical Engineering
Purdue University
West Lafayette, IN

Issued June 1994
August 1993

Sponsored by:
U.S. Department of Commerce
Ronald H. Brown, *Secretary*
Technology Administration
Mary L. Good, *Under Secretary for Technology*
National Institute of Standards and Technology
Arati Prabhakar, *Director*

Notice

This report was prepared for the Center for Fire Research of the Building and Fire Research Laboratory of the National Institutes of Standards and Technology, under Grant Number 60NANB1D1172. The statements and conclusions contained in this report are those of the authors and do not necessarily reflect the views of the National Institutes of Standards and Technology, the Building and Fire Research Laboratory, and the Center for Fire Research.

AN INVESTIGATION OF OIL AND GAS WELL FIRES AND FLARES

by

P. DUTTA, Y.R. SIVATHANU AND J.P. GORE

Thermal Sciences and Propulsion Center
School of Mechanical Engineering
Purdue University
West Lafayette, IN

FINAL REPORT: Grant No. 60NANB1D1172

August 1993

Sponsored by

U.S. DEPARTMENT OF COMMERCE

NATIONAL INSTITUTE OF STANDARDS AND TECHNOLOGY

BUILDING AND FIRE RESEARCH LABORATORY

CENTER FOR FIRE RESEARCH

EXECUTIVE SUMMARY

A theoretical and experimental study of jet flames with applications to large fires resulting from oil well and gas well accidents is reported. The results have been used in the interpretation of the single point radiative heat flux data collected around well fires in Kuwait. Based on the high liquid loading involved in actual well fires, a new device called effervescent atomizer/burner was successfully designed, constructed and tested during the grant period. Measurements of flame heights, radiative heat loss fractions, emission temperatures, and path integrated transmittances were completed for nine crude oil + methane/air flames in the 10-20 KW range.

The significant accomplishments during the grant include: (1) development of a technique to find total radiative heat loss from turbulent jet flames based on measurements of heat flux at a single location. This technique has already been applied by NIST investigators in Kuwait and is also being used by other US and international laboratories; and (2) design and successful operation of an effervescent atomizer/burner. This design and operation explained some of the mechanisms by which high liquid loading (up to 95% by mass) two phase jets may sustain turbulent diffusion flames. The burner also allows laboratory measurements of such flames for the first time; (3) study of global properties of the high liquid loading jet flames have shown that their lengths are affected by two-phase flow effects and that their soot loading and radiant output is lower than equivalent pool flames.

The first time opportunity to study high liquid loading jet flames in the laboratory has led to a study with applications in the industrial safety and insurance-cost containment areas. Design of liquid handling and storage systems, areas around storage tanks and pipes, and fire safety and fire fighting procedures and effectiveness will benefit from the laboratory information concerning fire size, shape and radiant output.

List of Figures

List of Figures (Cont.)

TABLE OF CONTENTS

CHAPTER I

INTRODUCTION

The objectives of the work reported in the following report were to gain an improved understanding of structure and radiation properties of oil and gas well fires particularly those involving large liquid fuel loading. The overall work can be separated into two major parts. The first part involved the determination of a relationship between radiative heat flux measured at a specified location around a jet flame and its total radiant output. The work on this problem had an urgent practical application during the early part of the grant. This application involved positioning of the limited heat flux gauges during the planned measurements in the Kuwaiti oil fields and interpretation of the results. The second part of the study involved development and operation of a high liquid loading atomizer/burner for studying the laboratory counterparts of the oil well fires.

The work completed in finding a relationship between single point radiative heat flux and total radiant output involved a study of scaling relationship between these quantities, the total heat release rate, the flame height and the geometric coordinates of the heat flux gauge. The propriety of the scaling relationship and the required constants in this relationship were obtained using data for 23 flames reported in the literature. Six additional flames were studied during the present investigation as well. Furthermore, the basis for the existence of the simple scaling relationship was examined by completing calculations of flame structure and radiation heat flux using a modified k-ε-g and a modified multi-ray discrete transfer program. The details of this part of the project are described in Chapter II which is a copy of a manuscript that recently appeared in *Combustion and Flame*.

Chapter III describes an investigation motivated by a question regarding how effervescent atomizers (which were traditionally developed for operation with air) would respond to the use of methane (which has a lower molecular weight) as an atomizing gas. The results of this work

showed that the atomization quality actually improves somewhat with a reduction in the molecular weight. The chapter is a copy of a paper that has been revised as per reviewer's comments for possible publication in the *ASME Journal of Fluids Engineering*.

Based on the encouraging performance of the atomizer, an atomizer/burner was constructed. The performance of this burner and global properties of the high liquid loading jet flames stabilized on it are described in Chapter IV. A study of flame heights has shown that two-phase effects are important in high liquid loading spray fires. The jet fires also appear to produce lower soot volume fractions and resultant radiative flux compared to pool flames burning Alberta sweet crude oils. These issues will be investigated for crude oil and other industrial liquids such as heptane and toluene during a proposed project.

Chapters II through IV each have their separate nomenclature, main sections, tables, figures, and references following the stand-alone nature of the work described in them. Chapter V is a concise discussion of the major conclusions reached based on the project and an outline of the work that is recommended for the future.

CHAPTER II

Total Radiative Heat Loss in Jet Flames from Single Point Radiative Flux Measurements

Y. R. Sivathanu and J. P. Gore
School of Mechanical Engineering
Thermal Sciences and Propulsion Center
Purdue University
W. Lafayette, IN 47907

ABSTRACT

A method for estimating total radiant output of turbulent jet flames based on the measurement of radiative heat flux at a single location is reported. The radiative flux from a variety of jet flames was measured and plotted in normalized coordinates to establish the feasibility of this approach. In addition, the radiative flux from acetylene/air diffusion flames to representative detector locations, for two different burner geometries and flow conditions, was calculated using the Planck-averaged equation of transfer coupled with a multi-ray technique. The local temperature and soot volume fractions for the calculations were obtained from emission/absorption measurements. The normalized calculated heat flux for the two flames also collapse with the experimental data. This result shows that scalar property distributions combined with the appropriate view factor for the single location are the basis for the single point technique.

NOMENCLATURE

C_o Constant for radiative flux calculations

C^* Ratio of total radiative flux to that estimated from single point radiance measurement and isotropic assumption

(Appeared in Combustion and Flame, Vol. 94, No. 3, pp. 265-270, 1993)

d	diameter of burner
E_e	Total energy emitted by a segment along the radiation path
f_v	Soot volume fraction
H_c	Lower heating value of the fuel.
I_e	Total intensity emitted by a segment along the radiation path.
i_λ	Spectral radiation intensity
L_{fv}	Visible length of the flame
m	Mass flow rate of fuel
Q_f	Heat release rate
q_r	Radiative heat flux at any location
Q_{Rad}	Total energy radiated to the surroundings
R	Detector distance radially outward along the exit plane of the burner
Re	Reynolds number based on exit conditions, $Re=U_o d_o/\nu_o$.
T	Temperature
x	Height of detector above injector exit parallel to the axis of the jet
X_R	Fraction of chemical energy lost to the surrounding by radiation.

Greek

δs	Length of segment along the radiation path
ε_p	Planck-mean emissivity
λ	Wavelength
ν	Kinematic viscosity of fuel
σ	Stefan's constant
ω	Solid angle

INTRODUCTION

The total energy radiated by fires to the surroundings is of importance in determining burning rates, flame spread and evaluating safety standards for buildings and materials. The fraction of chemical energy that is radiated to the surroundings (X_R) is defined as,

$$X_R = Q_{Rad}/Q_f. \quad (1)$$

Q_{Rad} is the total energy radiated to the surroundings and $Q_f = mH_C$, where m is the fuel flow rate and H_C is the lower heating value of the fuel. Experimentally, X_R is found to be a characteristic of the fuel over a range of operating conditions with relatively long residence times [1-4].

Some of the values of radiative fractions, X_R, reported in the literature have been based on Eq. (1) with Q_{Rad} obtained by integration of the radiative flux, q_r, over a 'semi-infinite' cylindrical enclosure surrounding the flames [2-6]. The measurements of q_r are carried out along the base of a cylinder at the exit plane of the burner and parallel to the axis of the flame until the radiative flux decreases to the low measurement limit of the gauge. Since measurements of the distribution of radiative flux over such an enclosure are not always feasible, many estimates of radiative heat loss fractions have been made from single point measurements and an assumption of spherical isotropy [1, 7-8].

Modak [9] suggested a formula for single location radiance measurement for pool fires based on a simple analysis using global flame properties. The formula based on simplifying assumptions such as constant absorption-emission coefficients, uniform radiation temperature and time

averaged flame shape provide reasonable estimates of X_R in optically thin pool flames. However, for optically thick pool flames, Hamins et al. [10] showed that the estimates based on Modak's analysis [9] were not consistent with the measurements and could lead to errors as high as 50%. Hamins et al. [10] have experimentally shown that a single measurement of heat flux can provide a reasonable estimate (within 13%) of X_R for liquid pool fires, if the location for this measurement is chosen at approximately half the flame height and at least five times the pool radius from the pool center.

For jet flames, the single point prescription of Hamins et al. [10] would lead to significant difficulties as 5 times the jet radius is very close to the flame boundary and could for certain conditions be located within the flame envelope. The shape of jet flames is substantially different from that of pool flames. The present paper is the first study of radiative heat flux from jet flames aimed at determining a single location that yields the total radiant energy.

For large scale flames, such as the Kuwait oil-well fires, the only locations for which radiative flux can be measured are at ground level. For such applications, the radiative fraction needs to be estimated from a single point radiative flux measurement at an appropriate point in the plane the burner.

Based on the above observations, the objectives of the present work are: (1) to propose a technique for the evaluation of radiant output of jet flames from a measurement of heat flux at a single point; (2) to examine

the efficacy of the technique using existing and new experimental data; and (3) to study the basis for the estimation of radiative fraction using a single point heat flux measurement.

SCALING REQUIREMENTS

Figure 1 shows a sketch of a turbulent jet flame together with the geometric distances that influence the radiation heat flux, q_r, incident at a detector location. The important distances are: x - the height of the detector above the plane of the fuel injector, R - the distance of the detector from the axis of the flame, and L_{fv} - the visible flame height. In addition, the heat flux is influenced by the chemical energy released in the flame, Q_f, and the fraction of this energy radiated to the surroundings, X_R. If the measurement of q_r at the location x, R is to be adequate for estimating the X_R then the three non-dimensional parameters formed using the above variables must be relevant to the problem. i.e.

$$\frac{q_r 4\pi R^2}{Q_f X_R} = C^*\left(\frac{x}{L_{fv}}, \frac{R}{L_{fv}}\right), \qquad (2)$$

where C^* determines the functional dependence of the parameter involving the q_r, X_R, and Q_f on x/L_{fv} and R/L_{fv}. If the function C^* is independent of burner diameter, fuel flow rate and the type of the fuel, it can be used in conjunction with measurements of q_r at a location x, R to determine $Q_f X_R$. Furthermore, if Q_f is known then X_R can be found from the above information. Evans and coworkers [11] have also used this technique to find Q_f for very large jet flames in Kuwait based on a reasonable approximation for X_R of crude oil/methane flames.

EXPERIMENTAL DATA

Some of the past measurements of q_r [3, 12] did not document the parameter R/L_{fv}. Other measurements of q_r [4, 5] did not involve a systematic variation of R to keep the parameter R/L_{fv} fixed while studying the influence of x/L_{fv} on C^*. Therefore, new measurements of q_r at $R/L_{fv}=0.5$ for six different flames burning CH_4, C_2H_2 and C_2H_4 as representative fuels were completed. The axial location of the detector was varied from the burner exit until the radiative heat flux reached 5% of the peak value. This location typically varied between 1.5 and 2.5 times the visible flame height. Measurements of q_r at x=0 with detector facing vertically up as a function of the radial distance from the injector exit were also completed in order to obtain the measurements of X_R for the six flames. As discussed later, the function C^* inferred from these measurements was found to collapse within 15% for certain x/L_{fv} locations. Such locations are ideal for the measurement of q_r to obtain total radiant output of the flame. In order to seek the basis of this collapse, the function C^* was also obtained from the heat flux calculations described in the following.

MULTI-RAY RADIATION CALCULATIONS

The function C^* was evaluated for acetylene/air flames using the calculations of q_r based on a multi-ray method similar to Refs. [2, 3, 6, 13]. Acetylene/air flames with two injector diameters of 6 mm and 12.5 mm, and heat release rates of 18.2 kW and 56.5 kW were selected since the radiative heat loss from these are very high ($X_R \simeq 60\%$). Furthermore, since the radiative properties are dominated by continuum radiation from

soot particles, gas band radiation can be neglected. Effects of scattering by soot particles and agglomerates on radiative heat flux have also been found to be small [14].

The radiation heat flux incident on the detector is the weighted sum of the heat flux incident from the different rays shown in Fig. 1. The heat flux contributed by the different rays is evaluated as the product of the radiation intensity and the fraction solid angle intercepted by the ray.

The radiation intensity incident from a representative path S in Fig. 1 is evaluated by integrating the discretized equation of transfer. The ray is divided into N homogenous segments with length ΔS, temperature T, and soot volume fraction f_v. For continuum radiation from soot particles, the instantaneous total energy, E_e emitted by a homogeneous segment, J along a radiation path [15] is

$$E_e\,(J) = 4 \int \int i_\lambda \, d\lambda \, d\omega = C_o f_v T^5, \qquad (3)$$

where i_λ is the spectral radiation intensity, $d\omega$ the differential solid angle, f_v the local soot volume fraction, and T the local temperature. C_o is a constant that depends on the refractive indices of soot and similar to past work [15], it is taken to be equal to $2.77*10^{-7}$ $kW/m^3/K^5$. Following Siegel and Howell [16], the intensity emitted by the segment J, $I_e(J)$, is

$$I_e(J) = E_e(J)\delta s/4\pi = \varepsilon_p(J)\sigma T(J)^4/\pi, \qquad (4)$$

where ε_p is the Planck-mean emissivity, δs the path length, and σT^4 is the blackbody emissive power. To account for the effects of turbulence on absorption and emission properties, the time averaged emitted energy and

blackbody emissive power are needed.

The equation of radiative heat transfer is numerically integrated using the following algorithm for a minimum of 22 rays [13] incident on the detector location as shown in Fig. 1. For each ray,

$$\bar{I}\,(J+1) = \bar{I}_e\,(J+1) + \bar{I}\,(J)\,(1-\varepsilon_p\,(J+1)), \qquad (5)$$

where $1-\varepsilon_p$ is treated as the Planck-mean transmitivity obtained from the time averaged Eq. (4). The resulting intensity incident on the detector (Fig. 1) is multiplied by an appropriate weighting factor and added to obtain the normal heat flux, q_r. The weighting factors are the fraction of area on the surface of a hemisphere of unity radius intercepted by the individual ray multiplied by the cosine of the angle between the normal to the detector surface and the incoming ray. The approximate Planck-mean emissivity method described above provided results that were within 20% of a spectrally resolved integration of the equation of radiative heat transfer.

In order to complete the calculations, distributions of mean emission intensity, absorptivity and incident energy at all points within the radiating volume of the flame are needed. In order to avoid the complexity of the soot kinetics and coupling between radiation, temperature and reaction processes within the flames, measurements of temperature and soot volume fractions were used to calculate the mean emissive power and absorptivity of individual segments. Such measurements are available from Refs. [5,17].

RESULTS AND DISCUSSION

Figure 2 shows the measurements and predictions of C^* ($=4\pi R^2 q_r / Q_f X_R$) plotted as a function of x/L_{fv} for a fixed value of R/L_{fv} (=0.5). Experimental data for three different fuels and heat release rates varying by an order of magnitude approximately collapse on one curve. The data appear to collapse particularly well near the peak heat flux location (x/L_{fv} between 0.5 and 0.7). The values of C^* estimated from the multi-ray analysis of the two acetylene/air flames also agree with the experimental data reasonably well. Based on these results, it is clear that measurements of radiative heat flux at x/L_{fv} = 0.5 - 0.7 and R/L_{fv} = 0.5 would yield an estimate of the total radiant output of the flame with C^* = 0.85. Based on the agreement between the measurements for various fuels and predictions, it is also clear that the distributions of temperature and soot volume fractions (or concentrations of other participating species) combined with the view factor for various rays lead to the scaling observed in Fig. 2.

It is observed that a range of x/L_{fv} near the location of maximum radiation heat flux yield similar values of C^* indicating some insensitivity to position in this region. With this information, the experimental data from the literature for which L_{fv} is not known or R/L_{fv} is not maintained constant can be utilized to estimate C^* approximately.

Table 1 shows experimental data from Refs. [3-5, 16] for 23 different jet flames burning eight different luminous and non-luminous fuels. The R/L_{fv} for some of these data varied between 0.6 and 1. Based on the measurements of q_r and X_R reported in the original references, a

value of C^* was calculated. For the data from Refs. [3, 16], the peak value of q_r was used in the calculations since measurements of L_{fv} are not available. The mean value of C^* from the 23 data is 0.90 with a standard deviation of 0.076. This value of C^* is higher than that obtained from Fig. 2 since the R/L_{fv} for these data were greater than 0.5. Thus, measurements of q_r near $x/L_{fv} = 0.5$ together with C^* between 0.85 and 0.90 can be used in conjunction with Eq. (2) to determine the radiant output of jet flames within 20%. From isotropic considerations, the value of C^* must be unity for very large values of R/L_{fv}, as the flame would effectively be a point source at such large distances.

The above single point technique has been applied to a study involving more than 50 jet flames by Turns and Myhr [18] to study the relationship between radiative loss fraction and NO_x production. For such studies that involve a large number of operating conditions and fuels, the present technique provides a simple method for measuring the radiative heat loss fractions.

For very large flames (such as those in Kuwait oil fields), it may not be practical to place a detector at half the flame height [11]. The only possible location for radiative flux measurements for such flames would be along the base of the flame for different radial positions. To examine the feasibility of using a single point measurement for such cases, the radiative heat flux to radiometers positioned at an angle of 45^o as shown in Fig. 1 was measured. Figure 5 shows the experimental data of normalized heat flux as a function of the radial distance for various fuels and operating

conditions taken for this study. There is much greater scatter among the data points, however, at a distance of roughly one flame height, the results suggest that it is feasible to use a single point along the base to determine the total heat flux from the flames within 30% with $C^* = 0.85$

CONCLUSIONS

Based on observation of experimental data for jet diffusion flames burning a wide range of fuels and from calculations for a single fuel and two operating conditions, a method of estimating the total radiation energy leaving jet flames from a single point heat flux measurement has been developed. The similarity in the distributions of scalar properties combined with the geometrical view factors of the specific detector location are the contributing factors to the existence of such locations.

ACKNOWLEDGMENTS.

This study is supported by the National Institute of Standards and Technology under Grant No. 60NANB9DO834 and Grant No. 60NANB1D1172 with Dr. D. D. Evans serving as NIST Technical Officer. The research program at NIST is supported by the Mineral Management Service, US Department of Interior with Mr. Ed Tennyson and Mr. Charles Smith serving as Technical Officers.

Table 1: Results of Single Location X_R test.

Fuel[a]	d (mm)	R/L_{fv}	$Q_f * X_R/4\pi R^2$ (kW/m^2)	q_r (kW/m^2)	C^*
Gore [3]					
Carbon Monoxide	5	-	0.46	0.38	0.83
Carbon Monoxide	5	-	0.52	0.48	0.93
Hydrogen	5	-	0.30	0.30	1.00
Hydrogen	5	-	0.50	0.45	0.90
Ethylene	5	-	1.17	1.15	0.99
Ethylene	5	-	2.27	1.90	0.84
Acetylene	5	-	1.44	2.00	0.72
Acetylene	5	-	2.57	3.10	0.83
Sivathanu [4]					
Acetylene	5	0.99	3.19	2.90	0.91
Acetylene	5	0.99	1.80	1.40	0.78
Ethylene	5	0.64	2.60	2.57	0.99
Ethylene	5	0.69	1.70	1.56	0.92
Ethylene	5	0.82	0.89	0.85	0.95
Propylene	5	0.61	4.26	3.83	0.90
Propylene	5	0.81	2.82	2.45	0.87
Propylene	5	1.01	1.61	1.25	0.78
Dolinar [5]					
Acetylene	6	0.87	2.44	2.26	0.93
Acetylene	6	0.84	2.93	2.90	0.99
Acetylene	12	0.86	5.50	5.05	0.92
Skinner [12]					
Methane	6	-	1.1	1.0	0.91
Methane/Acetylene[b]	6	-	2.8	2.8	1.00
Methane/Acetylene[c]	6	-	2.2	2.1	0.95
Acetylene	6	-	3.2	3.2	1.00

a Commercial Grade injected vertically upwards in still ambient air.

b A mixture of 27% methane and 73% acetylene by weight.

c A mixture of 57% methane and 43% acetylene by weight.

REFERENCES

[1] Markstein G. H., Twentieth Symposium (International) on Combustion, The Combustion Institute, Pittsburgh, 1984, p. 1055.

[2] Faeth, G. M., Gore, J. P., Chuech, S. G. and Jeng, S. M., Ann. Rev. Numerical Fluid Mech. and Heat Trans., (C. L. Tien and T. C. Chawla, eds.), Hemisphere, New York, 1989, p. 1.

[3] Gore, J. P., Ph. D. thesis, The Pennsylvania State University, University Park, PA, 1986.

[4] Sivathanu, Y. R., Ph. D. thesis, The University of Michigan, Ann Arbor, MI, 1990.

[5] Dolinar J., M. S. thesis, Mechanical Engineering Department, The University of Maryland Baltimore County, Baltimore, MD, 1992.

[6] Jeng, S. M. and Faeth, G. M., J. Heat Trans. 106:886-888 (1984).

[7] Becker, H. A. and Liang, D., Combust. Flame 44:305-318 (1982).

[8] McCaffrey, B. J., Western Section Technical Meeting, The Combustion Institute, Paper No. WSS/CI 81-15, 1981.

[9] Modak, A. T., Combust. Flame 29:177-192 (1977).

[10] Hamins, A., Klassen, M., Gore, J. and Kashiwagi, T., Combust. Flame 86:223-228 (1991).

[11] Evans, D. D., Personal Communications (1992).

[12] Skinner, S. M., M. S. Thesis, Mechanical Engineering Department, The University of Maryland, College Park, MD, 1991.

[13] Gore, J. P., Sivathanu, Y. R., and Ip. U. S., J. Heat Trans. 114:487-493 (1992).

[14] Mital, R., Sivathanu, Y. R., and Gore, J. P., Spring Technical Meeting of the Central States Section, The Combustion Institute, pp. 388-393, (1992).

[15] Gore, J. P., and Jang, J. H., J. Heat Trans. 114:234-242 (1992).

[16] Siegel, R., and Howell, J. R. "Thermal Radiation Heat Transfer," Hemisphere Publishing Corporation, New York.

[17] Sivathanu, Y. R, Dolinar, J. and Gore, J. P., Combust. Sci. Technol. 76: 45-67 (1991).

[18] Turns, S. R., and Myhr, F. H., Combust. Flame 87:319-335 (1991).

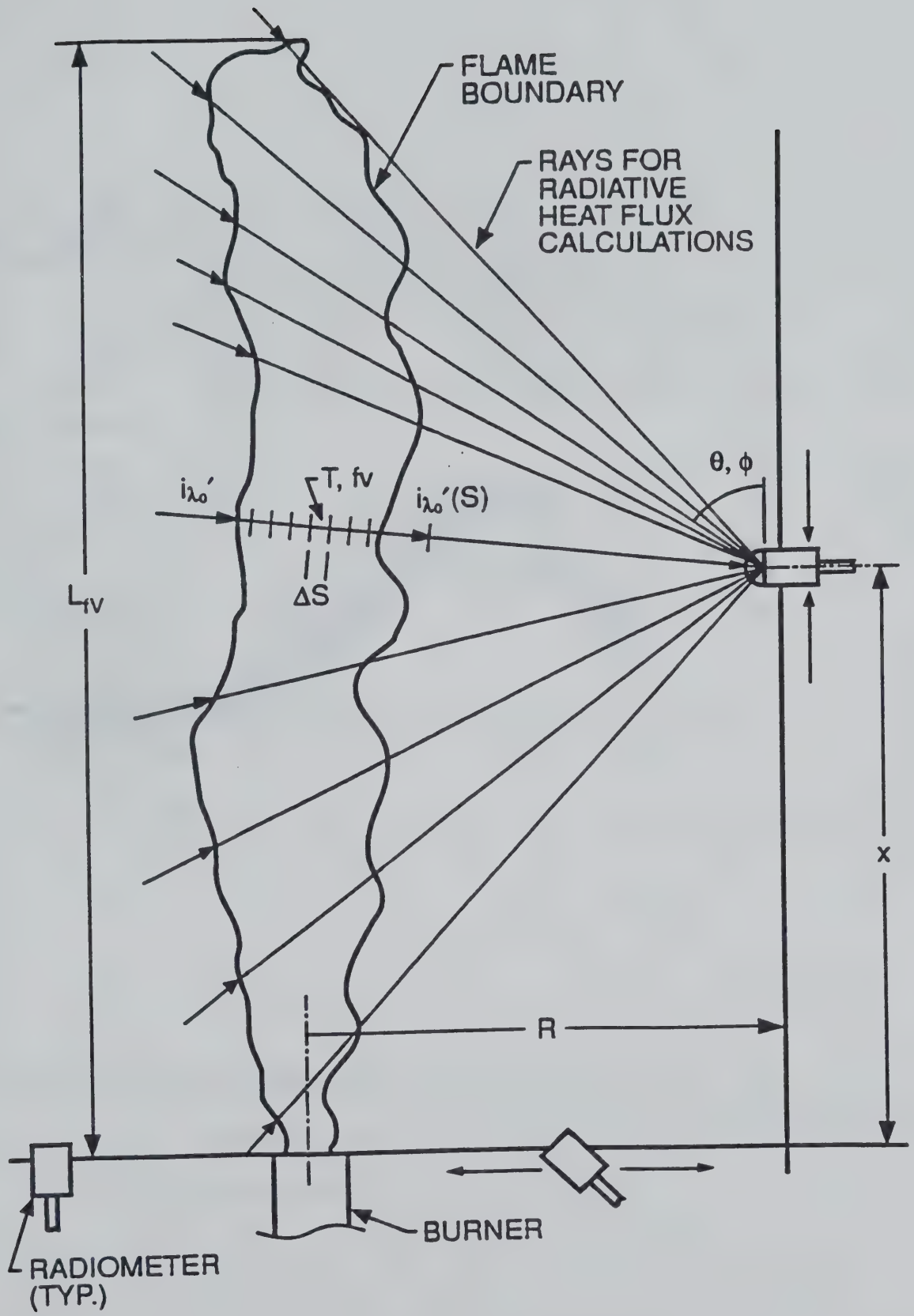

Fig. 1. Sketch of the flame geometry and the multi-ray radiation calculations.

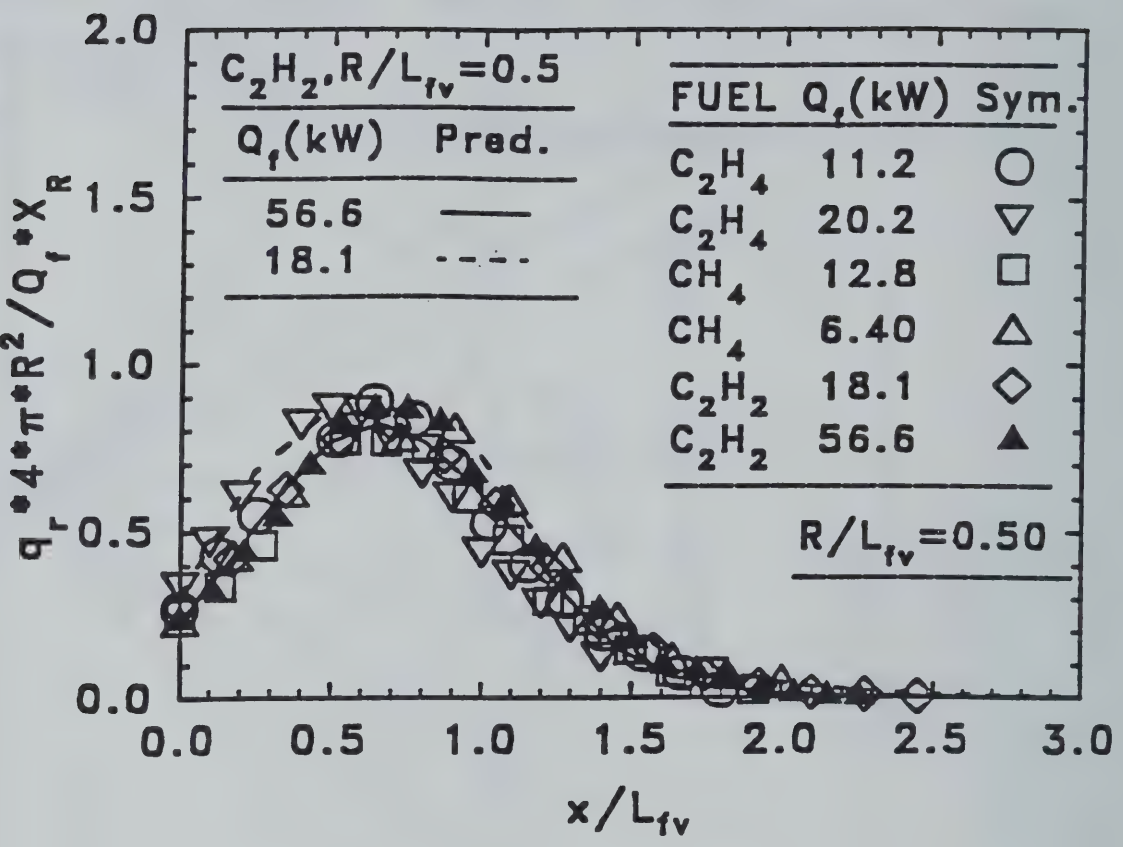

Fig. 2. Measurements and predictions of normalized radiative heat fluxes.

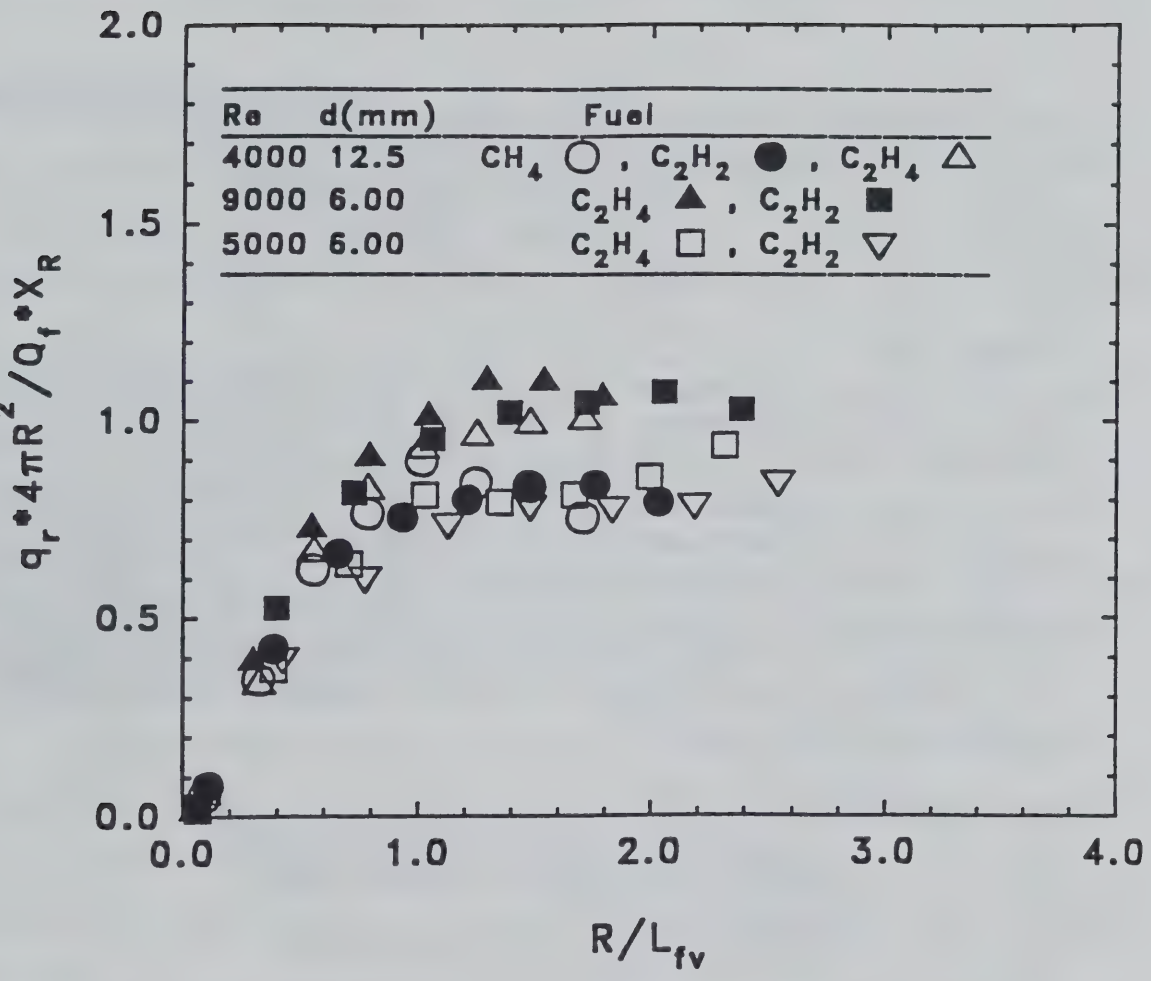

Fig. 3. Normalized radiation heat flux at the level of the fuel injector with 45^{o} detector orientation.

CHAPTER III

THE INFLUENCE OF ATOMIZING GAS MOLECULAR WEIGHT ON LOW MASS FLOWRATE EFFERVESCENT ATOMIZER PERFORMANCE

M.T. Lund,* C.Q. Jian, P.E. Sojka, J.P. Gore and M.V. Panchagnula**
Thermal Sciences and Propulsion Center
School of Mechanical Engineering
Purdue University
West Lafayette, Indiana 47907-1003

ABSTRACT

The relationship between atomizing gas molecular weight and spray mean drop size, Rosin-Rammler distribution parameter, and number averaged drop velocity is reported for a low mass flowrate effervescent atomizer-produced spray. Experimental data at lower gas-liquid ratios (GLR's) demonstrate that an increase in the molecular weight of the atomizing gas increases mean drop size and decreases number averaged drop velocity. The increase in mean drop size is attributed to an increase in the thickness of the liquid annulus at the nozzle exit and a subsequent increase in the diameter of ligaments formed there. The decrease in number averaged velocity results from a decrease in jet momentum flux. A model developed to explain the atomization process indicates that the gas flow is choked at higher GLR's.

NOMENCLATURE

C	A constant in the gas-phase momentum equation
C_{fi}	Interfacial friction coefficient, dimensionless
d	Diameter, m
GLR	Gas-to-liquid ratio by mass, dimensionless
$\dot{m}$	mass flowrate, kg/s
MW	Atomizing gas molecular weight, kg/kg-mole
p	Pressure, Pa
R_u	Universal gas constant, J/kgmole-K
sr	Gas-liquid velocity slip ratio, dimensionless
T	Temperature, K
α	Void fraction, dimensionless
μ	Viscosity, kg/m-s
ρ	Density, kg/m^3
σ	Surface tension, kg/s^2

---

* Currently with Procter & Gamble, Cincinnati, OH
** Currently with Vortec Corp., Philadelphia, PA

(Revised for possible publication in ASME Journal of Fluids Engineering)

Subscripts

g	Gas
l	Liquid
L	Ligament
o	Nozzle exit orifice

INTRODUCTION

Effervescent atomization studies have been reported by a number of researchers, with topics considered ranging from the influence of nozzle geometry and liquid physical properties on mean drop size to the structure of the spray. For instance, Wang et al. (1987) and Lefebvre et al. (1988) demonstrated that atomizer performance is independent of injector geometry and final orifice diameter while Roesler and Lefebvre (1989) reported that nozzle performance is nearly independent of mixing tube porosity. Buckner and Sojka (1991) showed that mean drop size is independent of viscosity for Newtonian liquids while Buckner and Sojka (1993) report no consistent variation in mean drop size with consistency index or flow behavior index for power law non-Newtonian liquids.

More recently, in a study closely related to this one, Lund et al. (1993) showed that an increase in surface tension reduces mean drop size, while an increase in viscosity leads to a slight increase in SMD. Lund et al. then developed a simple analytical model based on liquid and gas continuity, liquid and gas momentum conservation, annular flow at the nozzle exit (supported by their high speed photographs), and Weber's (1931) model for ligament breakup in order to explain the observed mean drop size versus surface tension and viscosity behavior.

A companion paper by Lund and Sojka (1993) discusses the spatial structure of low mass flowrate effervescent atomizer produced sprays. These authors indicate that the increase in mean drop size with an increase in distance from the spray centerline results from a droplet size dependent competition between inertia and drag, which allows the larger drops to penetrate farther in the radial direction. They also show that the increase in mean drop size with axial distance from the nozzle is due to turbulent mixing within the spray cone.

Finally, Lee and Sojka (1993) report a marked decrease in nozzle performance for viscoelastic liquids. They concluded that fluid relaxation time is the rheological parameter that controls mean drop size.

Each of the previous studies was concerned with nozzle performance when using air as the atomizing gas. While air would be the most common choice, there are applications where an atomizing gas other than air is desirable. An obvious example is a combustor where dual fuel operation is required; a relatively heavy oil would be the primary fuel and methane the atomizing gas and pilot fuel. A less obvious example is the two-phase jet that exits a ruptured oil well, with the Kuwait fires being a case in point. Here, crude oil and gases (usually some mixture of methane, ethane and propane) exit the well head in a two-phase stream and burn when ignited. Because of the size of an operating well head, such fires are impossible to reproduce in the laboratory and difficult to investigate in the field. Fortunately, a sub-scale model of an oil well fire can be

constructed using a low mass flowrate effervescent atomizer with a crude oil feed rate of 0.5 g/s providing a manageable firing rate of about 30 kW (Dutta et al., 1993).

Shifting from air to methane as the atomizing gas may influence mean drop size in the dual fuel combustor case and therefor impact combustion efficiency, pollutant formation, radiation heat transfer to the walls, and soot formation through variations in evaporation rate. In addition, when natural gas is used to atomize the oil, there will be variations in chemical composition that may lead to unacceptable swings in combustor performance if the molecular weight of the atomizing gas has a strong effect on nozzle performance. The composition of gas exiting an uncapped crude oil well head will vary from well to well so the influence of atomizing gas molecular weight on mean drop size is of interest to those simulating oil well fires.

These two applications motivated the present study into the influence of atomizing gas molecular weight on effervescent atomizer performance. These applications also motivated the choice of crude oil as the liquid to be sprayed and the low mass flowrates (0.5 g/s and below).

The following sections present the results of this study in terms of (i) Sauter mean diameter (SMD) and Rosin-Rammler distribution parameter (q) versus atomizing gas molecular weight (MW) at varying levels of gas-to-liquid ratio by mass (GLR) and for a crude oil mass flowrate, and (ii) number averaged drop velocity versus atomizing gas molecular weight, again for a single crude oil mass flowrate. The experimental data are then compared to predictions provided by a model based on the one developed by Lund et al. (1993) in order to explain why a change in gas molecular weight influences effervescent atomizer performance.

EXPERIMENTAL APPARATUS

The effervescent atomizer and liquid supply system of Lund et al. (1993) were used throughout this study. A schematic of the nozzle is provided in Fig. 1.

Alberta Sweet crude oil was chosen as the liquid to be sprayed because of its obvious application to oil well fires and because it is representative of residual fuel oils that might be burned in a dual fuel application. Alberta Sweet crude oil has a viscosity of 0.005 kg/m-s (5 cP), a surface tension of approximately 0.03 N/m (30 dynes/cm), and a density of 816 kg/m^3.

Atomizing gas was supplied using the system shown in Fig. 2. It consists of a pair of high pressure gas cylinders that supply helium and carbon-dioxide to a cylindrical stainless steel mixing chamber, with rotameters and metering valves included in each gas line to independently control the mass flowrates. The gas mixture was then routed to the injector's atomizing gas port.

Gas mixture molecular weights were varied between 8, half that of methane, and 44, that of propane, to span the range of possible (i) well head fire gas components and (ii) gas-phase fuels typical of combustion systems. Real gas effects were determined to be negligible by showing that the He and CO_2 compressibility factors were within 3% of unity for all conditions considered here.

A Malvern 2600 particle size analyzer was used to obtain line-of-sight number

density based drop size data while an Aerometrics Phase/Doppler Particle Analyzer (P/DPA) was used to collect complementary flux based drop size data and velocity distributions. The Malvern was employed because it facilitates rapid collection of nozzle performance data. Malvern results can, however, suffer from inaccuracies due to droplet size-velocity correlations. For that reason P/DPA data were also collected since results obtained using this instrument are not subject to drop size-velocity correlation related limitations.

All Malvern data were obtained using a 300 mm focal length lens and reduced by fitting the scattered light profile to a Rosin-Rammler drop size distribution. Results are reported as Sauter mean diameter and the Rosin-Rammler distribution parameter.

The P/DPA was fitted with a 495 mm transmitting lens and a 300 mm collimating lens and operated in the 30 degree forward scattering mode. This permitted measurement of drop diameters between 3.34 and 117 microns and axial velocities between 0 and 25 m/s. Validation rates were consistently above 90%. All P/DPA data are reported as either SMD or number averaged drop velocity.

Both P/DPA and Malvern data were collected on the spray axis at a point 150 mm downstream of the nozzle exit orifice. All data were acquired at room temperature, which was nearly constant at 293 K (68 F).

RESULTS

Representative results are shown in Figs. 3 through 6. Figures 3 and 4 present Malvern measured SMD and q versus molecular weight for GLR's ranging from 0.05 to 0.50. The crude oil mass flowrate is 0.5 g/s in all cases; GLR was therefor varied by adjusting the atomizing gas mass flowrate. Error bars are not included on these figures because they would be smaller than the symbols: the standard deviation relative to the mean is less than 4.0% for all the SMD data and less than 4.5% for all the q data.

The data demonstrate that mean drop size increases with atomizing gas molecular weight, although the magnitude of that increase diminishes as GLR increases from 0.05 to 0.50. In contrast, the width of the drop size distribution decreases slightly as molecular weight goes up. Finally, there is no systematic influence of GLR on the relationship between q and molecular weight.

The observation that mean drop size increases with atomizing gas molecular weight is supported by GLR=0.05 and 0.15 P/DPA measured mean drop size data presented in Fig. 5. Error bars are not included in Fig. 5 since the standard deviation relative to the mean for this data is always less than 4.0% and the error bars are therefor smaller than the symbols.

The disparity between Malvern and P/DPA measured SMD's is due to the two different methods used to sample the drops: the Malvern provides a number density based measurement and does not account for drop size-velocity correlations, whereas the P/DPA provides a flux based measurement and returns data that are therefor insensitive to drop size-velocity correlations.

Figure 6 shows that number averaged drop velocity decreases slightly with an increase in atomizing gas molecular weight and increases substantially with an increase in

GLR. The latter behavior was also observed by Lund and Sojka (1993) when using air as the atomizing gas. Error bars are not included in Fig. 6 since the standard deviation relative to the mean is less than 1.6% in all cases and the error bars are therefor smaller than the symbols.

Figure 7 provides a qualitative illustration of how changes in atomizing gas molecular weight shift spray mass between various size classes. The data are for a GLR of 0.15, however the behavior is indicative of all GLR's investigated. As can be seen, the width of the drop size distribution remains nearly unchanged, but mass is continually shifted from the larger drop categories to the smaller ones as atomizing gas molecular weight is reduced.

ANALYSIS

The mean drop size and velocity behavior illustrated in Figs. 3, 5 and 6 was analyzed using a modified version of the model developed by Lund et al. (1993). The Lund et al. model assumes that each ligament formed at the nozzle exit orifice behaves as a liquid jet with its fluid mechanic instabilities described by Weber's (1931) analysis. As such, the length of a ligament is assumed to correspond to the wavelength of the fastest growing disturbance

$$\lambda_{opt} = \sqrt{2}\pi d_L (1 + \frac{3\mu_l}{\sqrt{\rho_l \sigma d_l}})^{1/2} \qquad (1)$$

with each cylindrical ligament eventually forming a single spherical drop. Conservation of mass yields the following expression for the drop Sauter mean diameter

$$SMD = [\frac{3}{2}\sqrt{2}\pi d_L^3 (1 + \frac{3\mu_l}{\sqrt{\rho_l \sigma d_l}})^{1/2}]^{1/3} \qquad (2)$$

The ligament diameter, d_L, is found by first applying gas and liquid continuity to the annular flow at the nozzle exit orifice to determine the thickness of the liquid film there, then assuming that an integer number of ligaments exist in that film, and finally applying liquid continuity again to determine the ligament diameter.

Two key changes were made to Lund et al.'s original analysis. The first change was to include the effect of compressibility in the atomizing gas governing equations and was motivated by the fact that the gas phase Mach numbers exceeded 0.38 for all GLR's considered in this study. Lund et al. treated their gas phase as incompressible since their lower GLR's resulted in Mach numbers that were much lower than the ones considered here.

Gas phase compressibility was incorporated through a one-dimensional momentum equation

$$\frac{dp}{\rho_g} + V_g dV_g = 0 \qquad (3)$$

which was coupled with the ideal gas equation of state

$$p = \frac{\rho_g R_u T}{MW} \qquad (4)$$

While it is true that the gas flow at the nozzle exit is not truly inviscid, we have assumed inviscid flow for the gas phase momentum equation as a first approximation and included the interaction between the two phases at the interphase through the slip ratio expression.

The limiting thermodynamic paths, viz. adiabatic and isothermal expansion through the nozzle, were both considered. A comparison of predicted and measured drop sizes showed that the gas phase followed a thermodynamic path much closer to isothermal expansion than adiabatic. This is attributed to the intimate contact between the gas and liquid phases, which results in the liquid phase acting as a thermal reservoir for the gas.

Substituting Eqn. (4) into Eqn. (3), making use of the isothermal assumption, and integrating yields Eqn. (5)

$$\frac{R_u T}{MW} \ln\left(\frac{\rho_g R_u T}{MW}\right) + \frac{V_g^2}{2} = C \qquad (5)$$

where C is a constant.

The second change to Lund et al.'s model was to modify the slip ratio correlation originally proposed by Ishii (1977)

$$sr = \sqrt{\frac{\rho_l}{\rho_g}} \sqrt{\frac{\sqrt{\alpha}}{1+75(1-\alpha)}} \qquad (6)$$

to account for the influence of mass flow rate on velocity slip. Ishii's correlation was chosen by Lund et al. after their photographs of the region immediately upstream of the nozzle exit showed the presence of annular two-phase flow. The following paragraph provides justification for this change.

The parameter 75 in Equation (6) was originally introduced in a correlation developed by Wallis (1969) for the interfacial friction factor

$$C_{fi} = 0.005[1+75(1-\alpha)] \qquad (7)$$

Equation (7) was then used by Ishii when deriving his slip ratio expression for fully developed annular flow in pipes. In arriving at the value of 75, Wallis noted that the friction factor is a function of mass flow rate and that the slope of the C_{fi} versus $(1-\alpha)$ curve increases as the liquid mass flow rate increases. However, no quantitative

information was provided relating that slope to the liquid mass flowrate. Consequently, the value of 75 was scaled for the mass flowrates considered in this study.

The mass flowrate scaling was accomplished by matching predictions of mean drop size based on the model described here to the experimental SMD data of Lund et al. while varying the parameter 75. Mean drop size was calculated using Eqn. (2), which requires the measured liquid density, surface tension and viscosity, and the ligament diameter. The ligament diameter was determined via the approach discussed after Eqn. (2); this calculation requires the gas core diameter. The gas core diameter was determined from

$$\frac{\pi}{4}d_g^2 = \alpha\frac{\pi}{4}d_o^2 \qquad (8)$$

The void fraction is in turn related to the slip ratio, the (known) gas-to-liquid ratio, and the gas and liquid densities (Todreas and Kazimi, 1989)

$$\alpha = \frac{1}{1+\frac{sr\rho_g}{GLR\rho_l}} \qquad (9)$$

If Eqn. (5) is rewritten in terms of the known gas mass flowrate, the void fraction, and the gas density

$$\frac{R_u T}{MW}\ln\left(\frac{\rho_g R_u T}{MW}\right)+\frac{\dot{m}_g^2}{2(\rho_g\alpha\frac{\pi}{4}d_o^2)^2} = C \qquad (10)$$

Eqns. (6), (9) and (10) contain only three unknowns: α, ρ_g, and sr. They were solved iteratively using Newton's method.

Solution of Eqns. (6), (9) and (10) using the parameter value of 75 exhibited best agreement when compared to Lund et al's 0.8 g/s SMD data. Comparison of model predictions to data taken at 1.0 and 1.2 g/s indicated that the parameter value should be increased to 340 and 640, respectively. Note that an increase in the parameter value q with mass flowrate is consistent with Wallis' suggestion that the slope of the C_{fi} versus (1-α) curve should increase with $\dot{m}$.

Figure 8 illustrates the level of agreement between the experimentally obtained data of Lund et al. and model predictions that result from adjusting the Ishii parameter for the various mass flow rates. Error bars have not been included since the standard deviation relative to the mean is less than 5.6% with the result that the symbols are larger than the error bars in all cases.

The parameter values used to obtain the predictions presented in Fig. 8 were then extrapolated to the 0.5 g/s crude oil data collected during this study using a power law approach. A value of 10 was obtained. A comparison of model predictions (using the

value of 10) to the P/DPA data of Fig. 5 is presented in Fig. 9. It is limited to a GLR of 0.05 since the model indicates the gas flow chokes at higher values and sonic or supersonic flow cannot be treated by the current analysis. As Fig. 9 shows, qualitative agreement is achieved, with an increase in atomizing gas molecular weight leading to an increase in mean drop size. The model indicates that this behavior results from a five step process: (i) an increase in atomizing gas molecular weight increases the gas density; (ii) the increase in gas density in turn decreases the diameter of the gas core at the nozzle exit; (iii) the decrease in the diameter of the gas core increases the thickness of the liquid annulus; (iv) the increase in the thickness of the liquid annulus produces larger diameter ligaments at the nozzle exit; and (v) these larger diameter ligaments lead directly to larger drops (as shown in Figs. 3 and 5). The model also indicates why Fig. 6 shows a decrease in number averaged drop velocity upon an increase in atomizing gas molecular weight: raising the atomizing gas molecular weight reduces the velocity slip ratio. The decrease in velocity slip ratio leads to lower momentum fluxes at the nozzle exit, and therefor lower droplet velocities.

SUMMARY

An increase in atomizing gas molecular weight is shown to adversely affect the performance of a low mass flowrate effervescent atomizer by raising the mean drop size. A comparison of experimental data with predictions based on a modified version of the model of Lund et al. (1993) indicates that the increase in mean drop size results from a thickening of the liquid annulus as atomizing gas molecular weight is increased. Increasing the thickness of the liquid annulus leads directly to larger diameter ligaments at the nozzle exit and, hence, larger drops. An increase in atomizing gas molecular weight also decreases drop velocity. The model indicates that the observed decrease in drop velocity is due to a reduction in jet momentum flux at the nozzle exit. Finally, the model indicates the gas flow chokes for gas-liquid ratios much over 0.08.

Acknowledgments

The authors acknowledge the National Science Foundation's equipment grant for providing the Phase/Doppler Particle Analyzer used during this study, and the National Institute for Standards and Technology for financial support (CQJ and JPG). Dr. David D. Evans is the NIST grant monitor.

REFERENCES

Buckner, H.N. and Sojka, P.E., 1991, "Effervescent Atomization of High-Viscosity Fluids. Part I: Newtonian Liquids," *Atomization and Sprays*, vol. 1, pp. 239-252.

Buckner, H.N. and Sojka, P.E., 1993, "Effervescent Atomization of High-Viscosity Fluids. Part II: Non-Newtonian Liquids," *Atomization and Sprays*, vol. 3, pp. 157-170.

Dutta, P., Gore, J.P., Sivathanu, Y.R., and Sojka, P.E., 1993, "Global Properties of High

Liquid Loading Turbulent Crude Oil + Methane/Air Spray Flames," *Combustion and Flame*, revised.

Ishii, M., 1977, "One-Dimensional Drift-Flux Model and Constitutive Equations for Relative Motion Between phases in Various Two-Phase Flow Regimes," Argonne National Laboratory Rept. ANL 77-47.

Lee, W.Y. and Sojka, P.E., 1993, "The Influence of Fluid Viscoelasticity on Low Mass Flow Rate Effervescent Atomization," pp. 129-135 in Fluid Mechanics and Heat Transfer in Sprays, ASME FED-Vol.178/HTD-Vol. 270, J.W. Hoyt, T.J. O'Hern, C. Presser, A.K. Gupta, and R.L. Alpert, eds.

Lefebvre, A.H., Wang, X.F., and Martin, C.A., 1988, "Spray Characteristics of Aerated-Liquid Pressure Atomizers," *AIAA Journal Prop. & Power*, vol. 4, pp. 293-298.

Lund, M.T., Sojka, P.E., Lefebvre, A.H., and Gosselin, P.G., 1993, "Effervescent Atomization at Low Mass Flowrates. Part I: The Influence of Surface Tension," *Atomization and Sprays*, vol. 3, pp. 77-89.

Lund, M.T., and Sojka, P.E., 1993, "Effervescent Atomization at Low Mass Flowrates. Part II: The Structure of the Spray," *Atomization and Sprays*, submitted.

Roesler, T.C. and Lefebvre, A.H., 1989, "Studies on Aerated-Liquid Atomization," *International Journal Turbo and Jet Engines*, vol. 6, pp. 2221-230.

Todreas, N.E. and Kazimi, M.S. "Nuclear Systems I: Thermal Hydraulic Fundamentals," Hemisphere, New York.

Wallis, G.B., "One Dimensional Two Phase Flow", McGraw-Hill, New York.

Wang, X.F., Chin, J.S., and Lefebvre, A.H., 1987, "Influence of Gas Injector Geometry on Atomization Performance of Aerated-Liquid Nozzles," Heat Transfer in Furnaces, ASME HTD, vol. 74, pp. 11-18.

Weber, C., 1931, "Disintegration of Liquid Jets," *Z. Agnew. Math. Mech.*, vol. 11, pp. 136-159.

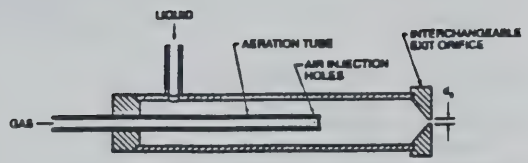

Fig. 1 Effervescent atomizer.

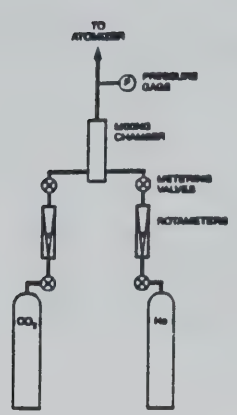

Fig. 2 Gas supply system.

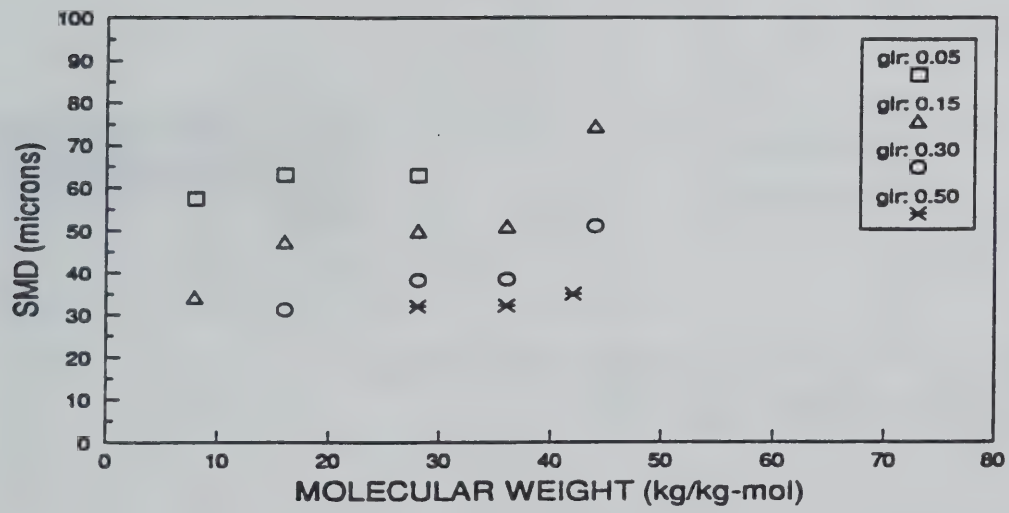

Fig. 3 Malvern measured Sauter mean diameter (SMD) versus atomizing gas molecular weight for four gas-liquid ratios (glr's).

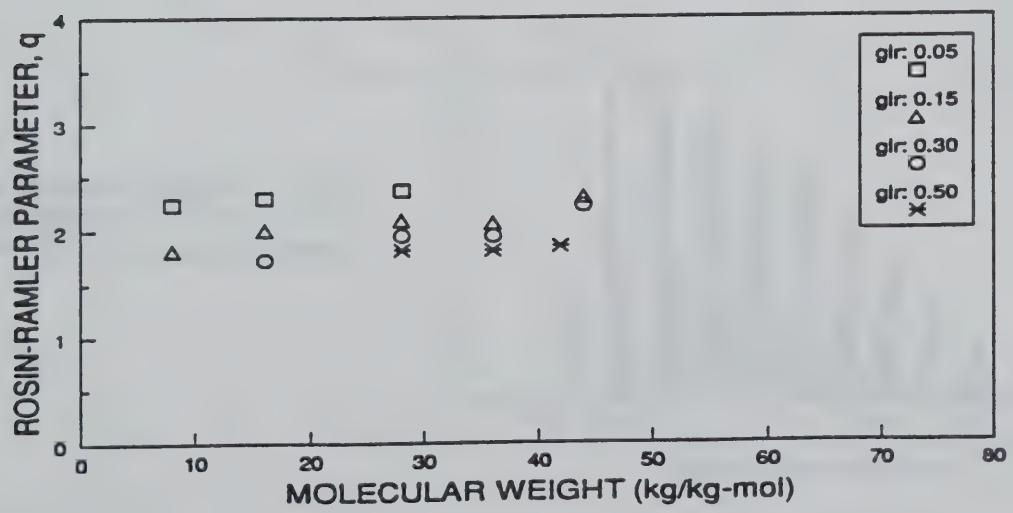

Fig. 4 Malvern measured Rosin-Rammler size distribution parameter (q) versus atomizing gas molecular weight for four gas-liqui ratios (glr's).

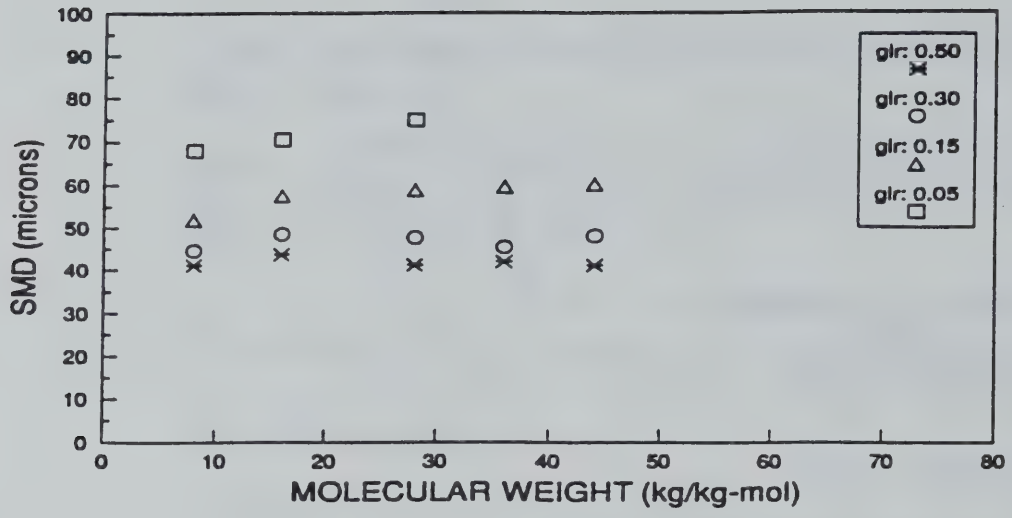

Fig. 5 P/DPA measured Sauter mean diameter (SMD) versus atomizing gas molecular weight for four gas-liquid ratios (glr's).

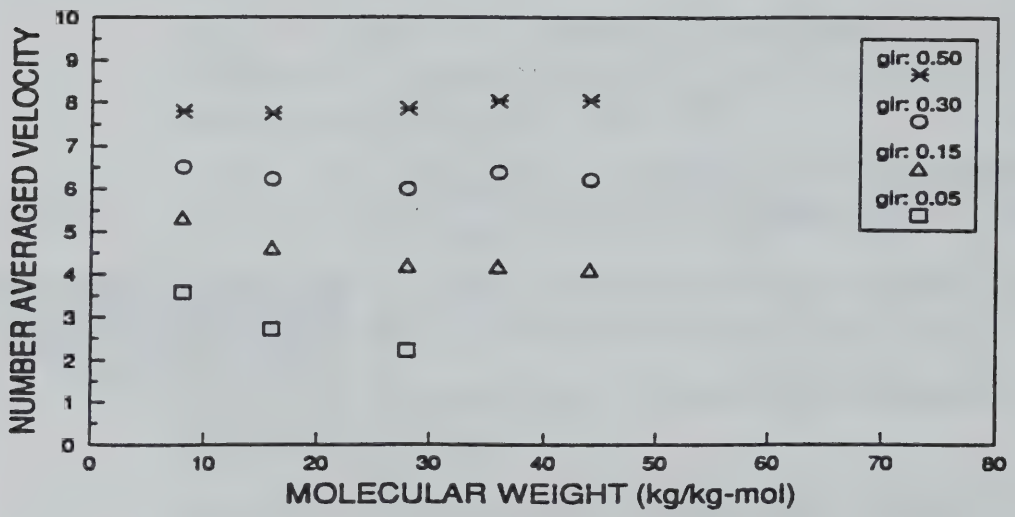

Fig. 6 Number averaged velocity versus atomizing gas molecular weight for four gas-liquid ratios (glr's).

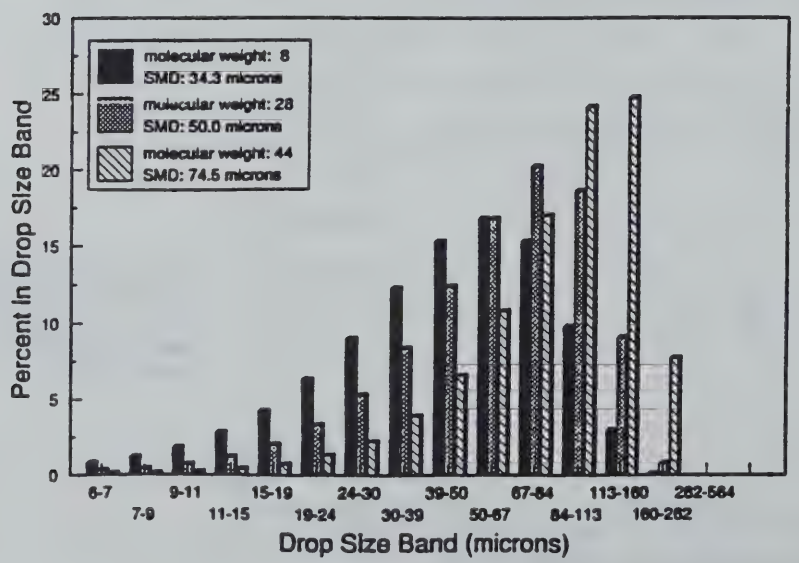

Fig. 7 Weight percent in each size band, for three different atomizing gas molecular weigh

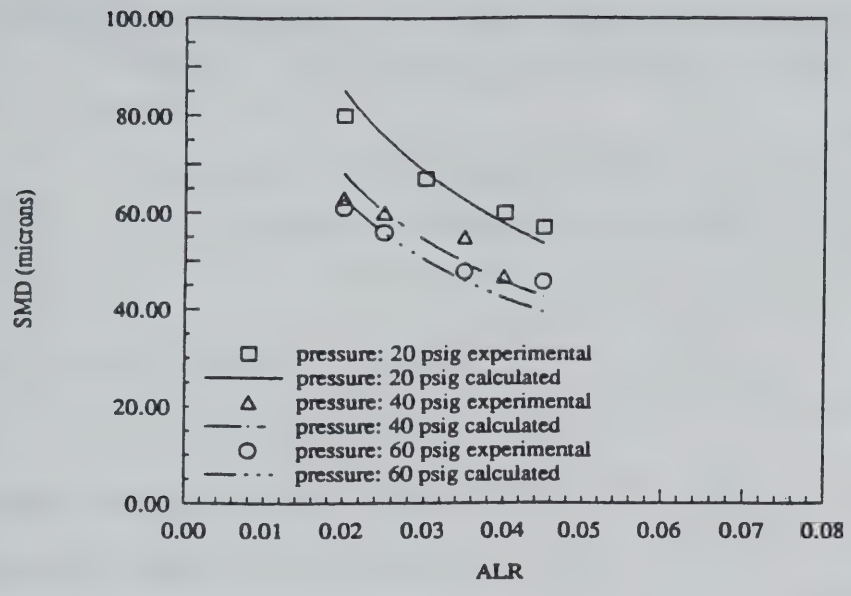

Fig. 8 Comparison of Lund et al. data with predictions using our model.

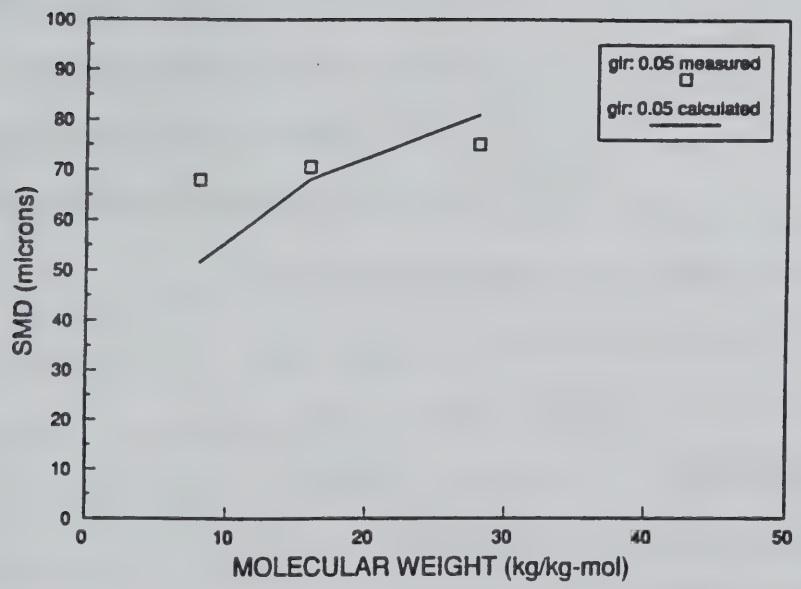

Fig. 9 Comparison of low ALR data from this study with predictions using our model.

CHAPTER IV

GLOBAL PROPERTIES OF HIGH LIQUID LOADING TURBULENT CRUDE OIL + METHANE/AIR SPRAY FLAMES

P. Dutta, J. P. Gore, Y. R. Sivathanu and P. E. Sojka
Thermal Sciences and Propulsion Center
School of Mechanical Engineering
Purdue University
West Lafayette, IN 47907

ABSTRACT

Measurements of atomization quality, flame heights, radiative fractions, emission temperatures, and transmittance for Alberta sweet crude oil/methane flames established on a novel burner for simulating well-blowout fires are reported. The results show the effects of two-phase flow on flame heights. The measurements of radiative fractions and the optical properties suggest relatively low soot loading. The measured high temperatures suggest almost complete combustion of crude-oil. However, larger-scale tests as well as information concerning the physical processes in the present atomizer and burner are essential for the application to practical fires and combustion devices.

NOMENCLATURE

d	External orifice diameter
g	Acceleration due to gravity
Fr	Froude number, $Fr = u^2/gd$
H_f	Visible flame height
HLR	Hydrogen-to-liquid ratio by mass
MLR	Methane-to-liquid ratio by mass
N	Rosin-Rammler drop-size distribution parameter
Q_f	Heat release rate
SMD	Sauter mean diameter

(Accepted for publication in Combustion and Flame)

u Nozzle exit velocity

x Distance from the nozzle exit

X Characteristic diameter in Rosin-Rammler distribution

X_R Fraction of chemical energy lost to the surrounding by radiation.

INTRODUCTION

Oil-well blowout fires during drilling, production or workover present a serious hazard to personnel, environment and equipment particularly on off-shore platforms [1, 2]. Typical oil-well blowout fires involve combustion of a mixture of liquid and gaseous fuels. The atomization of the liquid is caused by the expansion of the mixture to atmospheric pressure. Heat transfer from the combustion zone established by the gaseous components and the fuel vapor in conjunction with the atmospheric oxygen causes evaporation of the atomized liquid fuel. The infrared radiation energy leaving the resulting fires is hazardous to the platform, equipment and personnel.

Typically, material exiting an oil-well consists of 80 to 95% liquid with 20 to 5% gases and vapors by mass. In the absence of wind, the material expands in a vertical jet configuration, mixes with the surrounding air and forms turbulent jet diffusion flames stabilized at or above the well head. As previously observed in blowout fires and more recently in the oil-well fires in Kuwait, the liquid atomizes and evaporates effectively in this configuration and flames are stabilized. These jets represent high-liquid-loading dense sprays that have not been studied in the literature extensively [3].

The flame height, size, and radiation properties of high-liquid-loading two-phase flames have not received much attention in the literature except for the study of Hustad and Sonju [4], involving global property measurements for

relatively large-scale (1-8 MW) oil/gas flames. In that study, the oil and the gas were mixed in a chamber upstream of a large-diameter (10 mm - 33 mm) nozzle exit. In such a configuration, the quality of atomization changes with liquid loading and exit diameter. The measurements of visible flame heights by Hustad and Sonju [4] showed that the two-phase flames are much longer than gaseous flames with similar heat release rates. However, due to the large size of the flames, information concerning drop sizes and the extent to which the distance needed for evaporation of the fuel affected the flame heights could not be obtained.

Laboratory tests of two-phase spray flames have been restricted to relatively low-liquid-loading since conventional twin-fluid atomizers require high kinetic energy of the gas phase for effective atomization. Therefore, liquid mass fraction in the incoming stream has been restricted to 0.5 in past intermediate-scale and laboratory-scale tests [2, 5]. Attempts to increase the liquid loading resulted in large drops. A large amount of unburnt crude-oil also exited the flame due to lack of efficient evaporation. Therefore, an effervescent atomizer-burner was developed in the present study for the establishment of high-liquid-loading crude-oil jet flames in the laboratory.

In oil reservoirs, dissolved gases and light components exist in the form of small bubbles, which are similar to those found in effervescent atomizers. The high pressure oil-gas mixture exits from a long passage into an atmospheric pressure environment in oil-well fires, which is simulated by the effervescent atomizer-burner. Matching the conditions between the two any further would require detailed measurements of actual oil-well fires which are unavailable.

The effervescent atomizer concept and design followed the work of Lund et al. [6]. As discussed above, a study of the flames stabilized on this burner is

expected to improve the understanding of oil-well blowout fires due to the inherent similarity in the atomization and combustion processes.

A second limitation on the similarity between the laboratory and the practical oil-well flames is introduced by consideration of flame lift-off and blowout. Although lift-off and blowout characteristics of two-phase jet fires have not been studied, based on the work of McCaffrey and Evans [7] for gaseous jet flames it can be conjectured that the effects of burner size will be significant. McCaffrey and Evans [7] have shown that for natural gas-air flames, lift-off and blowout are observed with increasing exit velocity for tube diameters below 38 mm. This limit implies that all laboratory flames except those burning hydrogen or acetylene liftoff at velocities lower than those of practical interest in many applications. Laboratory studies of attached gaseous diffusion flames have therefore relied on pilot flames both non-premixed [8] and premixed [9] to overcome the lift-off and blowout problems. Similarly, the present two-phase laboratory jet fires must rely on a pilot flame which the practical oil-well blowout fires do not require.

The objectives of the present paper are: (1) to describe a successful design of the atomizer-burner; (2) to discuss global properties (visible flame height, radiative fractions) of the crude-oil/methane flames stabilized on the burner; and (3) to report path-integrated measurements of emission temperature and monochromatic transmittance to help understand the behavior of the radiative fractions. The present results for the visible flame height are also compared to the correlations of Hustad and Sonju [4] to highlight the effects of the atomization quality on the flame length.

EXPERIMENTAL METHODS

A sketch of the effervescent atomizer-burner is shown in Fig. 1. The effervescent atomization portion of the burner follows the design of Lund et al. [6] closely. The crude-oil flows into an annular space formed by the body of the burner and the central methane injection tube. The methane injection tube is similar to the aeration tube of Lund et al. [6]. Aeration is achieved by drilling multiple holes on the methane injector tube.

Small pool fires were observed around the oil-well fires in Kuwait. The crude-oil jet flames were stabilized by these small pool fires. In order to stabilize the flame on the burner port, a small ring flame of hydrogen is utilized. Use of a pool flame instead of a hydrogen ring would simulate an oil-well fire even more closely. The two-phase crude-oil-methane flow exits the central 0.38-mm orifice and flows through the ring flame resulting in a jet flame attached to the 4.76-mm diameter exit port of the burner. The top plate of the burner is cooled by a small flow of water flowing through an annular space to avoid fuel coking near the orifice.

Figure 2 is a schematic of the flow system used to control the pressures and the mass flow rates of crude-oil, methane and hydrogen flowing into the burner. The crude-oil is stored in a tank rated for 2 MPa. The liquid in the tank is pressurized using nitrogen connected to the gas space of the tank via a pressure regulator. The pressure in the tank is thus maintained by admitting nitrogen into the tank as the liquid is used. The liquid flow-rate is metered by a Nupro "S" series Fine Metering Valve. A shut-off valve is included so that the metering position can be maintained from one test to another. The flow-rate is monitored by a calibrated rotameter. The liquid pressure just upstream of the burner was monitored to be between 135-270 kPag using an inline pressure gauge for all the

tests reported here. The methane gas pressure upstream of the burner was between 205-410 kPag and the hydrogen pressure was approximately 138 kPag. The mass flow rate of methane is governed by a choked metering valve mounted downstream of a rotameter. The hydrogen flow is also monitored by a rotameter.

Table 1 shows the operating conditions for the flames studied during the present investigation. The mass flow rate of the atomizing methane varied between 5 and 20 % of the mass flow rate of the crude-oil. The Alberta sweet crude-oil has a density of 840 kg/m^3, viscosity of 5 cP, and surface tension of 30 dynes/cm [10]. The hydrogen flow used for flame attachment did not affect the atomization quality significantly and was maintained at 16.4 mg/s for all the flames except the last. In order to stabilize the flame with the highest crude-oil flow, a higher flow of hydrogen (21.2 mg/s) was required. The heat release rates for the flames varied between 9 and 21 kW based on nominal heating values of 43,400 kJ/kg for the crude oil, 50,000 kJ/kg for methane, and 120,900 kJ/kg for hydrogen. The Reynolds number characteristic of the jet were evaluated based on the external orifice diameter (4.76 mm) on which the flame is stabilized or based on the diameter through which the two-phase material exits (0.38 mm). The Reynolds numbers based on both these diameters are listed in Table 1. The use of the larger diameter assumes that the material expands to fill the exit port while the use of the smaller diameter assumes that the jet is formed independent of the external orifice. The two different assumptions lead to Reynolds numbers differing by an order of magnitude. The issue of the appropriate characteristic dimension is not currently resolved, as discussed later.

The radiative heat flux distribution from the flames to the surface of a long imaginary cylindrical enclosure with a base aligned at the level of the burner (semi-infinite cylindrical enclosure) was measured using a Medtherm wide angle

(150^{o}) radiometer. The resulting data were integrated to obtain the total energy radiated by the flames. The details of the measurement technique and the geometry of traverse of the radiometer have been discussed in detail by Sivathanu and Gore [11]. The uncertainties in these measurements are less than 10% based on the least count of the data acquisition system. The radiative fractions (X_R) obtained from these measurements are listed in Table 1. These vary from approximately 10% for the flames with the highest methane loading to approximately 20% for the flames with the highest crude-oil loading. These values are relatively low, indicative of highly forced jets. However, measurements of velocities are needed to clarify further the issue of momentum versus buoyancy effects.

The atomizer-burner was operated in a cold-spray configuration facing downward (injecting in the direction of gravity) to evaluate its performance in terms of drop-size distributions. A Malvern 2600 particle size analyzer with a focal length 300 mm was used for these tests similar to previous work [6,10]. The particle sizes were measured at a distance of 25 diameters (12 cm) downstream of the atomizer to ensure that most of the particles are spherical drops. Effects of total oil flow rate and methane-to-oil mass-flow-rate ratio (MLR) on drop size distribution were studied.

The flames were stabilized with the burner facing vertically up (opposing the direction of gravity) in a screened enclosure of 1m x 1m x 2m size with exhaust gas removal at the top. Past tests by Lund [12] have shown that the orientation does not affect the atomization quality. The vertically-up orientation is clearly preferred for the removal of the exhaust products as well as for simulating the actual oil-well fires. Flame heights were measured by first recording the flames using a charge coupled device (CCD) array video camera

with the shutter speed set at 1000 Hz. Heights were then measured from the video screen and averaged over 40 frames with a measurement taken every five frames. The frames were 1/60 th of a second apart. The video screen was appropriately scaled to provide actual flame heights. Uncertainties of the flame height measurements were found to be less than 7% based on the repeatability of the ensemble averages.

In order to examine the emission of smoke into the exhaust stream as well as understand the radiative fractions of different flames, measurements of path-integrated transmittance and path-integrated emission temperatures were obtained for diametric paths at various heights above the burner exit. The instrumentation used for these tests was developed by Sivathanu et al. [13]. However, instead of inserting the purged stainless steel probes into the flame, the entire flame was observed to obtain path-integrated absorption and emission data.

A helium-neon laser (632.8 nm wavelength) with a chopper was used to obtain the monochromatic transmittance of the flames. The transmittance of the flames is lower than unity due to absorption by soot particles and intermediate hydrocarbon species, as well as scattering and absorption by the liquid oil drops along the path. In the parts of the flame that contribute to significant flame radiation, the reduction in the transmittance is dominated by absorption due to soot particles. Emission at 900 and 1000 nm is measured by two calibrated photomultiplier tubes with optical filters (100 nm band-width at half-peak transmittance). The emission data are used to infer the global temperature assuming specific absorption coefficients of soot particles given by Dalzell and Sarofim [14] and incorporating the transmittance curve of the filters into the calculation. These values have been found satisfactory for obtaining emission temperature data [15]. Possible interference from emission by hydrocarbon

species other than soot particles was neglected as a first step. Experimental uncertainties inherent to the three-wavelength instrument are discussed in Ref. [13].

RESULTS AND DISCUSSION

Figure 3 shows the distribution of drop sizes measured by the Malvern analyzer at an axial location of x/d = 25 along the centerline of the spray for three different liquid flow rates with a fixed methane-to-liquid flow rate ratio (MLR). The measurement of x is obtained from the base of the burner on which the flame is stabilized, to the location in the flame where the Malvern beam or other instruments were positioned. The accuracy of the linear traverse used for measuring x is 1 mm. The measurements were made two times at every location and the typical change in the SMD was 3-4%, which is within the range of accuracy of the Malvern particle sizer. Each measurement consisted of 1000 sweeps over a period of 8 seconds. The data were fit to a Rosin-Rammler drop-size distribution [16]. The Rosin-Rammler distribution may be expressed in the form

$$1 - Q = \exp - (D / X)^N$$

where Q is the fraction of the total volume contained in drops of diameter less than D, and X and N are constants. The exponent N is a measure of the spread of drop sizes in the spray. The Rosin-Rammler parameters X and N are indicated on Fig. 3 for each drop-size distribution. The variation in X was between 2-8%, while the variation in N was between 2-12%. The effect of the changes in hydrogen flow rate were determined to be small (2 micron change in SMD over the flow rate range 0 to operating condition) by turning this flow rate off during the drop size measurements. This is within the range of accuracy of the Malvern instrument. The Sauter mean diameter (SMD), which is significant in

determining the evaporation rates, increases with the liquid flow rate between 260 mg/s and 360 mg/s but appears to stay almost constant between 360 mg/s and 400 mg/s. The resulting changes in evaporation length for the liquid drops may translate into differences in the visible flame heights as will be seen later.

It was observed previously [10] that the ratio of methane-to-oil mass-flow rates affects the drop size more significantly than the total liquid flow rate. Figure 4 shows the drop size distribution measured by the Malvern analyzer for a fixed heat release rate of the flame (Q_f = 14 kW) and varying methane-to-oil mass ratios. For a MLR of 5%, the drops have an SMD of 38.70 μm. This decreases to 26.90 μm as the methane flow rate is increased to 10% and then to 23.70 μm as the methane flow rate is increased further to 14%. It is therefore expected that the flame height will increase with decreasing methane-to-oil ratio (MLR).

Figure 5 shows the flame height "H_f" normalized by the external orifice diameter "d" (4.76 mm) plotted as a function of the total heat release rate for the first seven flames in Table 1. The last flame had a higher flow of hydrogen for stabilization and hence is not considered together with the others. As seen in Fig. 5, the flames are taller for lower methane loading. For the methane loading of 5%, the flame height increases with heat release rates. This is probably due to the longer evaporation length needed because of the 1) higher mass-flow rate of oil and 2) larger drop size produced at higher liquid-flow rates. The height of buoyant jet flames burning gaseous fuels also increases with heat release rate due to the slower relative air entrainment rates with the decreasing influence of buoyancy. Depending upon which one of the two characteristic diameters is appropriate, the present flames would be in the buoyant or the forced jet regimes. Measurements of velocities at the exit would clarify this question. However,

whether larger evaporation length affects flame lengths can be assessed by fixing the heat release rate and varying the liquid loading.

Figure 5 shows that for a fixed heat release rate of 14 kW, the flame height normalized by the external orifice diameter (4.76mm) decreases with increasing MLR. This is in agreement with the smaller drops created by the enhanced atomization with increasing MLR leading to a shorter evaporation length. It also suggests that the changes in flame height with heat release rates are partly due to the two-phase flow effects unique to spray flames.

Flame heights obtained from the correlation of Hustad and Sonju [4] for methane gaseous jet flames are also plotted in Fig. 5. For large methane flames, the correlation for the flame height is given by :

$$H_f/d = 21\ Fr^{0.2}$$

where Fr is the Froude number calculated from the two-phase velocity based on the external orifice diameter (4.76mm). As can be seen from the figure, a systematic variation of 20 to 40% exists for the different conditions. The Froude number has not been modified by the two-phase flow correction suggested by Hustad and Sonju [4]. If used, it would show even higher differences between measured values and the correlation. However, the velocity and the diameter used are based on the two-phase density and the total mass flow rate exiting the external orifice. In the work of Hustad and Sonju [4], the gas exit velocity was used to calculate the Froude number. For the present conditions, this would lead to very low flame heights. The constant 21 in the correlation may be adjusted due to differences in the fuel. However, the qualitative discrepancies in flame height variation would persist. The correlations of Becker and Liang [17] based on gas flames were also tried, but overpredicted the flame heights by up to a factor of 2.

Based on these observations, it is apparent that two-phase effects need to be considered in flame-height correlations for high-liquid-loading spray flames.

The radiative heat flux to a semi-infinite cylinder surrounding the flames was measured using a wide angle radiometer. The distance of the radiometer from the flame axis during the axial traverse was selected to be equal to the flame height H_f based on the scaling rule devised by Sivathanu and Gore [11]. The radiative heat flux was normalized by the total radiant output of the flame divided by the surface area of an imaginary sphere with radius equal to the distance from the detector to the flame axis. The normalized heat flux plotted as a function of the normalized axial distance is shown in Fig. 6. The data for the eight flames collapse extremely well on the plot of Fig. 6 suggesting that the radiation scaling of Sivathanu and Gore [11] is applicable to two-phase flames. The effects of different fuel properties (soot concentrations and temperature) are accounted for by the radiative fraction used in the scaling. The differences in geometry of the flame are accounted for by the use of the flame height. Therefore, the effects of two-phase flow are built into the scaling via the effects on flame height caused by different evaporation length requirements. As pointed out by Sivathanu and Gore [11] the collapse of Fig. 6 provides a convenient method for obtaining the total radiant output of a jet flame by making the radiation heat flux measurement at a single point.

As described in Table 1, the radiative fractions, X_R, vary between 10.2 % and 21.4 %. Figure 7a shows the X_R plotted as a function of the total heat release rate for a fixed MLR. The values of X_R are independent of the heat release rate for a fixed MLR. Figure 7b shows that X_R increases with decreasing MLR at a fixed heat release rate due to the propensity of crude oil flames to soot. The values of X_R are lower than expected. For buoyant methane jet flames, X_R values

of approximately 18% are reported in the literature (see [18] and their references), for pool flames burning Alberta sweet crude-oil a value of X_R=30% has been reported [5]. Thus the values of X_R for the present jet flames are unexpectedly low. Such low values can be realized if the flame temperatures are low due to incompleteness of combustion or if the sooting tendency of crude-oil is substantially diminished in the present flame configuration. These questions can be discussed with the help of the emission and absorption data.

Figure 8 shows the measurements of emission temperature and transmittance for flames with MLRs of 14%, 10% and 5%. These correspond to test cases 2, 4 and 5 respectively in Table 1. The heat release rate is maintained at 14 kW for all cases. The uncertainties in the mean temperature measurements were about 10%. This was estimated by perturbing the signals from the flame by the RMS of the measurements during black-body calibration. Since the measurements are path integrated, the temperature probe selects the peak temperature values along the path. For the highest methane loading the peak temperatures (see Fig. 8a) are approximately 2200 K near the injector exit and reduce to approximately 2150 K at approximately x/d=70 before decreasing beyond the flame tip. The small decrease in peak flame temperature is due to the relatively low radiative heat loss. The high peak temperatures represent almost complete combustion of the fuel. With increasing liquid loading, the peak temperatures decrease only slightly near the burner exit. For the lowest methane loading, the temperatures decrease by approximately 300 K with axial distance primarily due to radiative heat loss. The highest-liquid-loading flame shows emission due to soot until x/d=120. The reduction in temperature decreases some of the expected increase in radiant output due to reduced transmittance with higher liquid loading.

The decrease in transmittance of the diametric path is shown in Fig. 8b. The transmittance for the highest-liquid-loading flame decreases to approximately 0.6 while those for the intermediate and low-liquid-loading cases are much higher. The overall decrease in transmittance causes the total radiant energy for the high-liquid-loading flame to increase from 10.2 % to 21.4% (see Table 1) in spite of the reduction in temperature. The relatively high value of measured temperatures suggest that the reduced radiant loads are not due to incompleteness of combustion.

The basic reasons for reduced soot formation in the present spray configuration that contribute to reduced radiant heat loss are presently unknown. However, the basic understanding of soot formation and emission processes even in gaseous flames is such that the present work must be limited to reporting the first experimental observations for high liquid loading spray flames.

CONCLUSIONS

The following conclusions can be drawn from the present study:

(1) The effervescent atomizer-burner leads to efficient combustion in crude-oil/methane/hydrogen flames with very high liquid loading,

(2) The measurements of flame height showed systematic effects of liquid loading and atomization quality. The flame heights increase with increasing heat release rates and decreasing methane-to-liquid mass flow rate due to the longer distance needed for evaporation of the drops,

(3) The measurements of radiative fractions are unexpectedly low. Based on the emission temperature measurements, incompleteness of combustion does not play a role in the reduced radiative fractions. These data and relatively high measured transmittances suggest that reduced soot loading contributes to lower X_R,

(4) Single-point radiation measurements following the scaling rule of Sivathanu

and Gore [11] can be used to estimate the total radiant output for the two-phase flames,

(5) Study of additional operating conditions, particularly those with increased residence time, are needed to obtain generalized global properties for crude oil/methane flames.

ACKNOWLEDGEMENTS

This study was partially supported by the National Institute of Standards and Technology, Building and Fire Research Laboratory under Grant No. 60NANB1D1172 with Dr. D. D. Evans serving as NIST Scientific Officer. The work regarding oil well fires at NIST is supported by the Mineral Management Service of the US Department of Interior with Mr. Charles Smith and Mr. Ed Tennyson serving as Program Managers.

REFERENCES

1. Evans, D. D., and Pfenning, D., *Oil and Gas Journal* 83:No. 17, 80-86 (1985).

2. Gore, J. P., and Evans, D. D., OCS Study MMS 91-0057, (J. B. Gregory, C. E. Smith, and E. J. Tennyson, eds.), United States Department of Interior, Washington D.C., 1991.

3. Faeth, G. M., *Prog. Energy Combust. Sci.* 13:293-345 (1987).

4. Hustad, H., and Sonju, O. K., *Dynamics of Reactive Systems Part I: Flames and Configurations,* (J. R. Bowen and R. I. Soloukhin, eds.), Progress in Astronautics and Aeronautics Series, AIAA, New York, Vol. 105, 1986, p. 365.

5. Gore, J. P., Klassen, M., Hamins, A., and Kashiwagi, T., *Fire Safety Science Proceedings of The Third International Symposium,* (G. Cox and B. Langford, eds.), Elsevier Science Publishers Ltd., London, 1991, p.395.

6. Lund, M. T., Sojka, P. E., Lefebvre, A. H. and Gosselin, P. G., *Atomization and Sprays* 3:77-89 (1993).

7. McCaffrey B. J. and Evans D. D., *Twenty-First Symposium (International) on Combustion,* The Combustion Institute, Pittsburgh, 1986, p. 25.

8. Gore J. P., Ph.D. Thesis, The Pennsylvania State University, University Park, PA, 1986.

9. Masri A. R., and Bilger R. W., *Twenty-First Symposium (International) on Combustion,* The Combustion Institute, Pittsburgh, 1986, p. 1511.

10. Lund, M. T., Jian, C. Q., Sojka, P. E. Gore, J. P. and Panchagnula, M., *J. Fluids Engineering*, 1993, in revision for *ASME J. Fluids Engineering*. Also to be presented at the ASME Winter Annual Meeting 1993, New Oeleans.
11. Sivathanu, Y. R., and Gore, J. P., *Combust. Flame* , 1993 94:265-270 (1993).
12. Lund, M. T., MSME thesis, Purdue University, West Lafayette, IN, 1992.
13. Sivathanu, Y. R., Gore, J. P. and Dolinar, J., *Combust. Sci. Technol.* 76:45-66 (1991).
14. Dalzell, W. H., and Sarofim, A. F., *J. Heat Trans.* 91:100-104 (1969).
15. Sivathanu, Y. R., Gore, J. P., Janssen, J. M., Senser, D. W., *J. Heat Trans.* 115:653-658 (1993).
16. Rosin, P., and Rammler, E., *J. Inst. Fuel* 7:No. 31, 29-36 (1933).
17. Becker, H. A., and Liang, D., *Combust. Flame* 32:115-137 (1978).
18. Faeth, G. M., Gore, J. P., Chuech, S. G., and Jeng, S. M., *Ann. Rev. Numerical Fluid Mech. and Heat Trans.*, (C. L. Tien and T. C. Chawla, eds.), Hemisphere, New York, 1989, p.1.

Table 1: Operating Conditions.

Test Case	$\dot{m}_{OIL}$ (mg/s)	$\dot{m}_{CH_4}$ (mg/s)	MLR (%)	$Re_{d}{}^{a}{}_{=4.76mm}$	$Re_{d=0.38mm}$	Q_f (kW)	X_R (%)
1.	135	27.0	20	3.8×10^3	1.8×10^4	9.2	11.4
2.	234	32.8	14	5.5×10^3	2.3×10^4	14.2	10.2
3.	238	23.8	10	4.9×10^3	1.8×10^4	13.5	15.5
4.	250	25.0	10	5.1×10^3	1.9×10^4	14.0	14.0
5.	260	13.0	5	4.8×10^3	1.1×10^4	13.9	21.4
6.	328	16.4	5	5.4×10^3	1.3×10^4	17.0	20.7
7.	360	18.0	5	5.7×10^3	1.5×10^4	18.5	20.6
8.[b]	400	20.0	5	6.9×10^3	1.6×10^4	21.0	19.5

[a] $Re_d = \dfrac{\rho_{TP} V_{TP} d}{\mu_{TP}}$

[b] Higher hydrogen flow rate

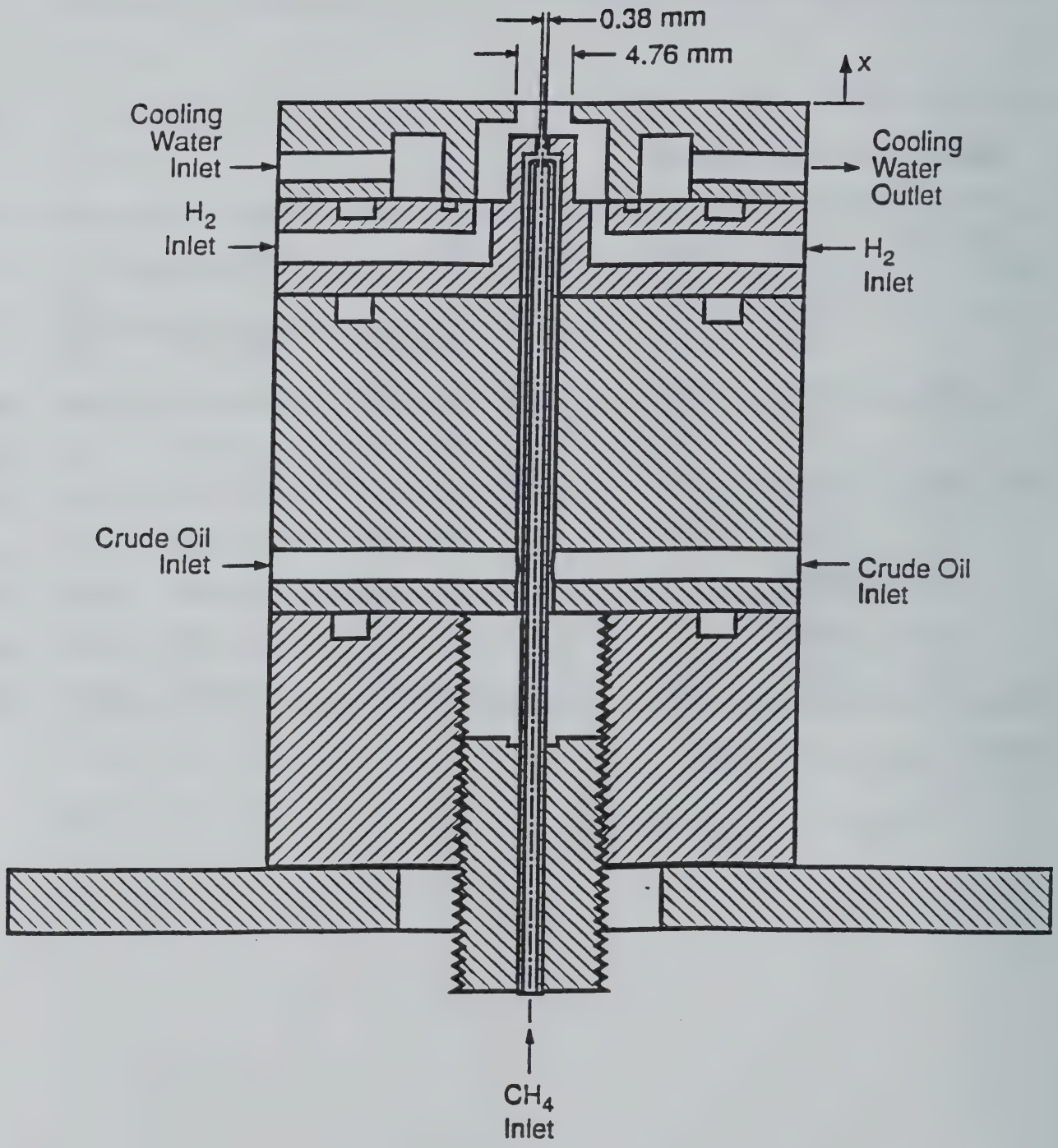

Fig. 1. Sketch of the effervescent atomizer-burner.

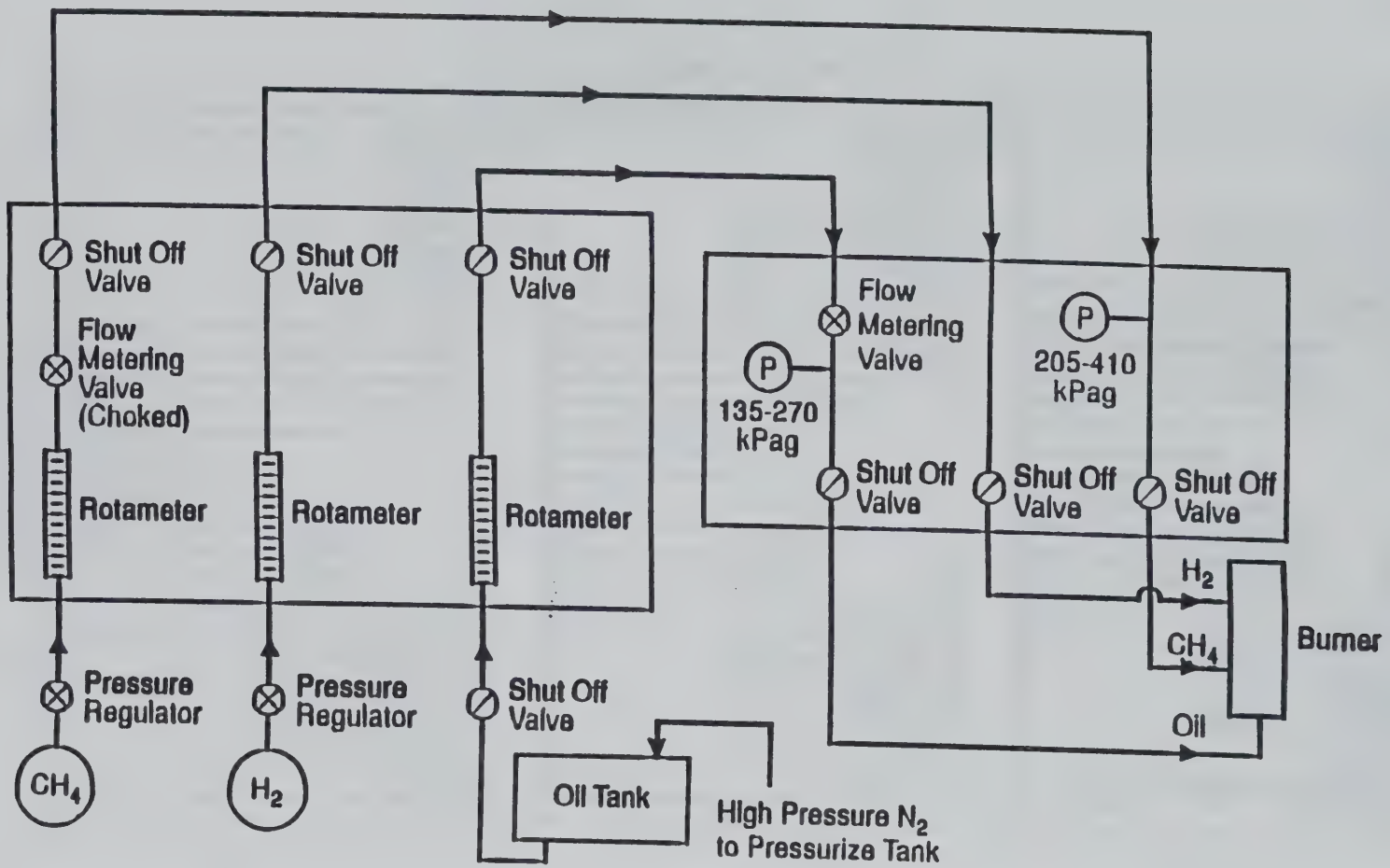

Fig. 2. Schematic of the flow control system for the effervescent atomizer burner.

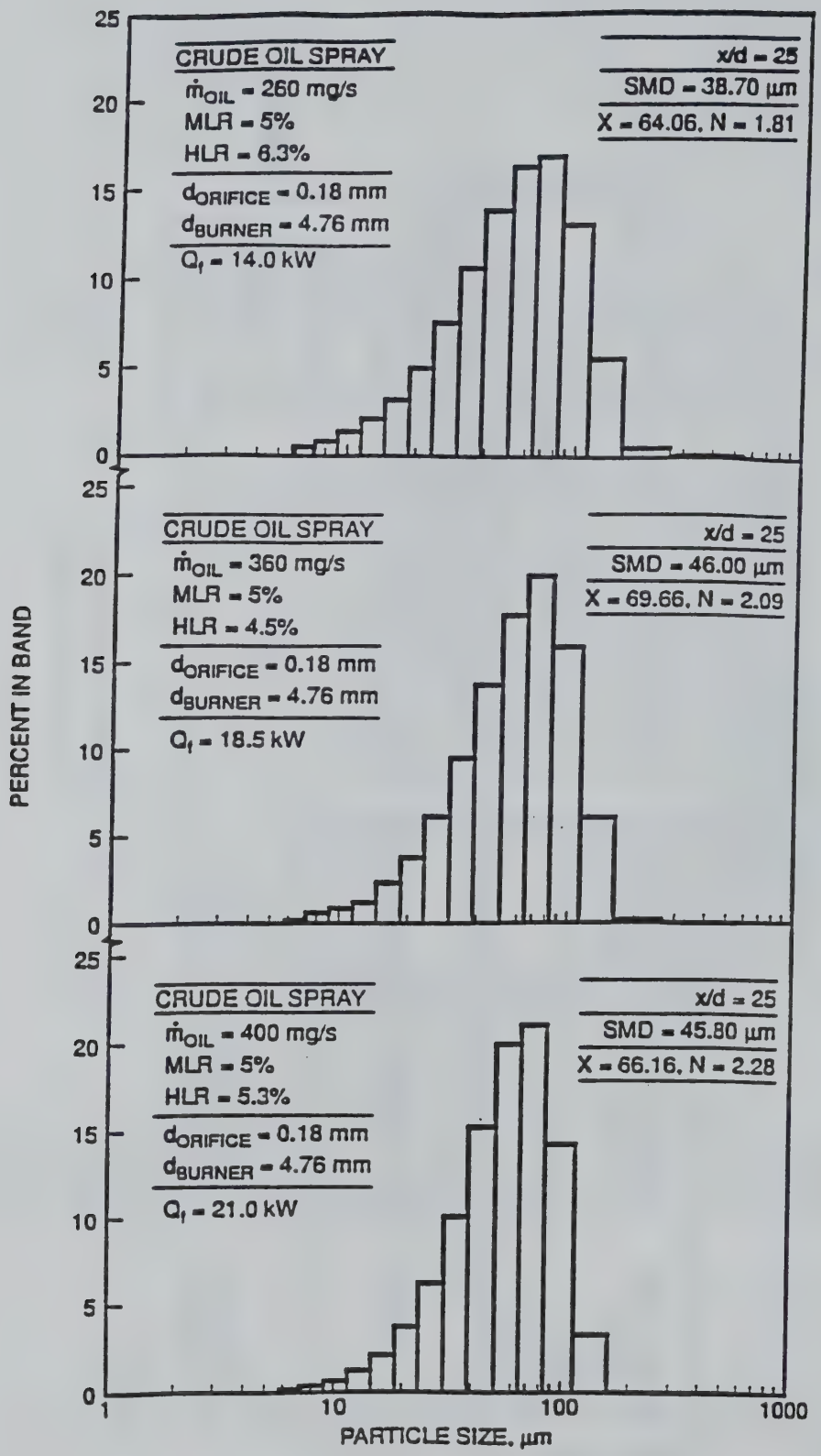

Fig. 3. Malvern measurements of drop size distributions for crude-oil sprays for three liquid flow rates with fixed methane-to-liquid ratio.

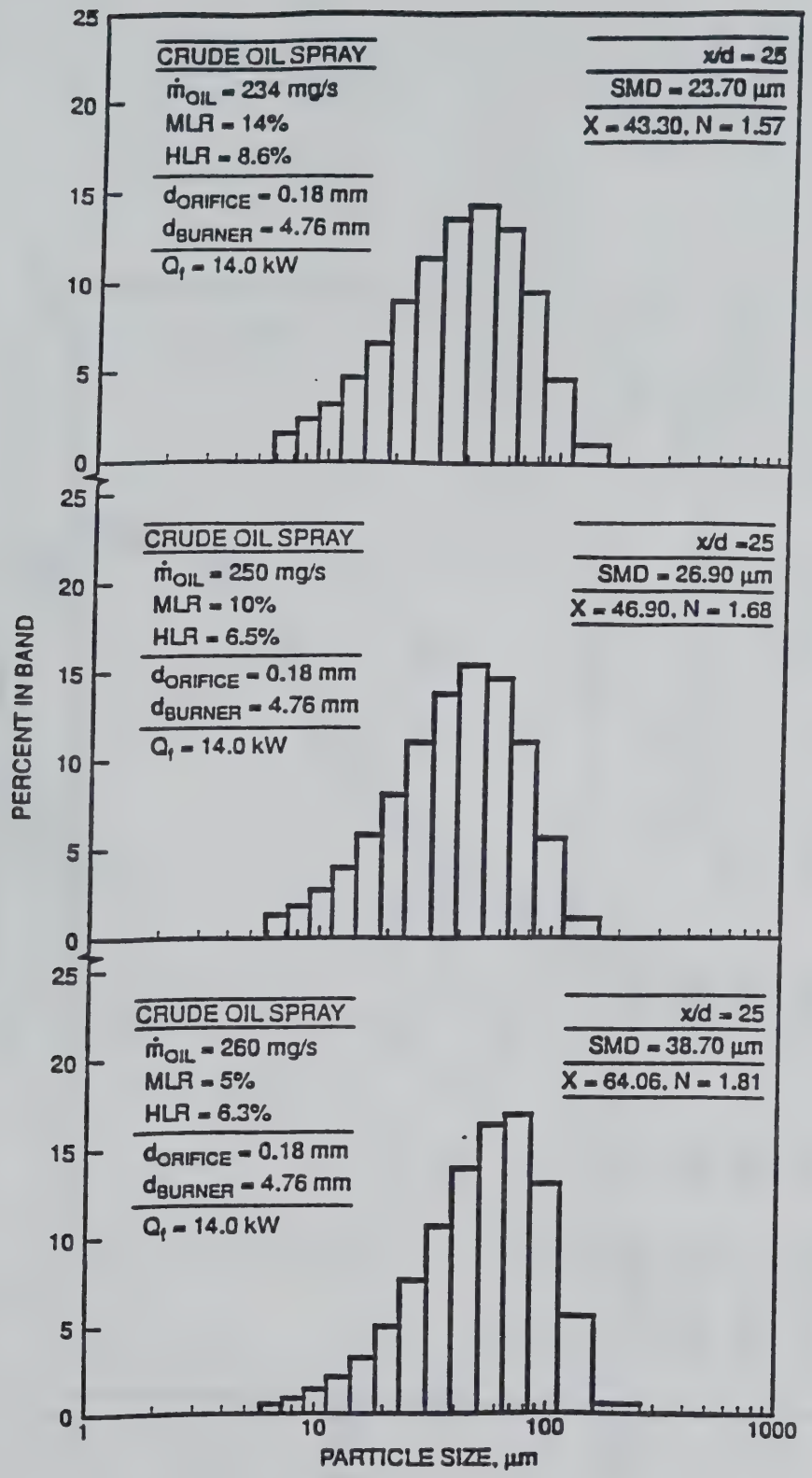

Fig. 4. Malvern measurements of drop size distributions for crude-oil sprays for three methane-to-liquid ratios with fixed heat release rate.

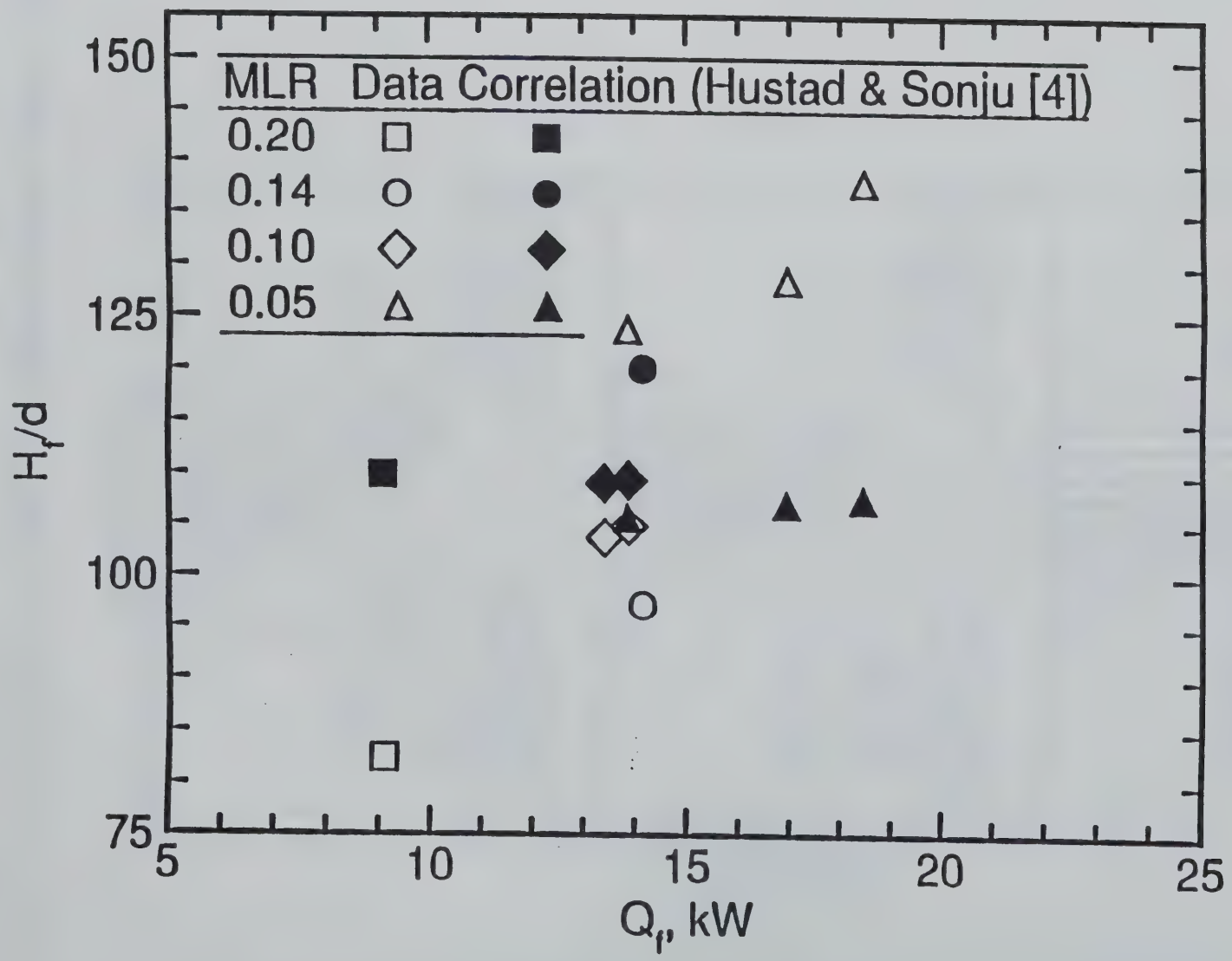

Fig. 5. Visible flame heights as a function of heat release rate for several methane-to-liquid ratios.

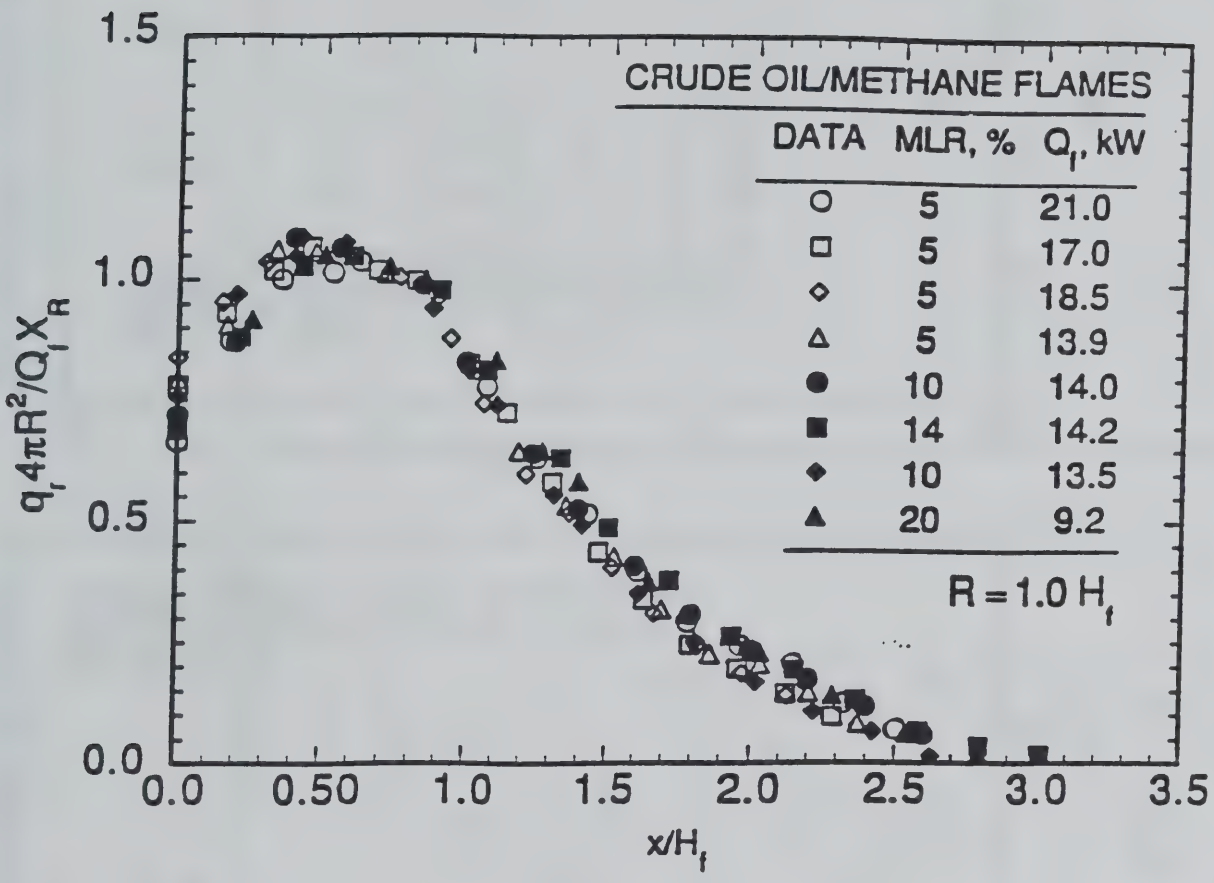

Fig. 6. Normalized radiative heat flux parallel to the axis of crude oil/methane flames.

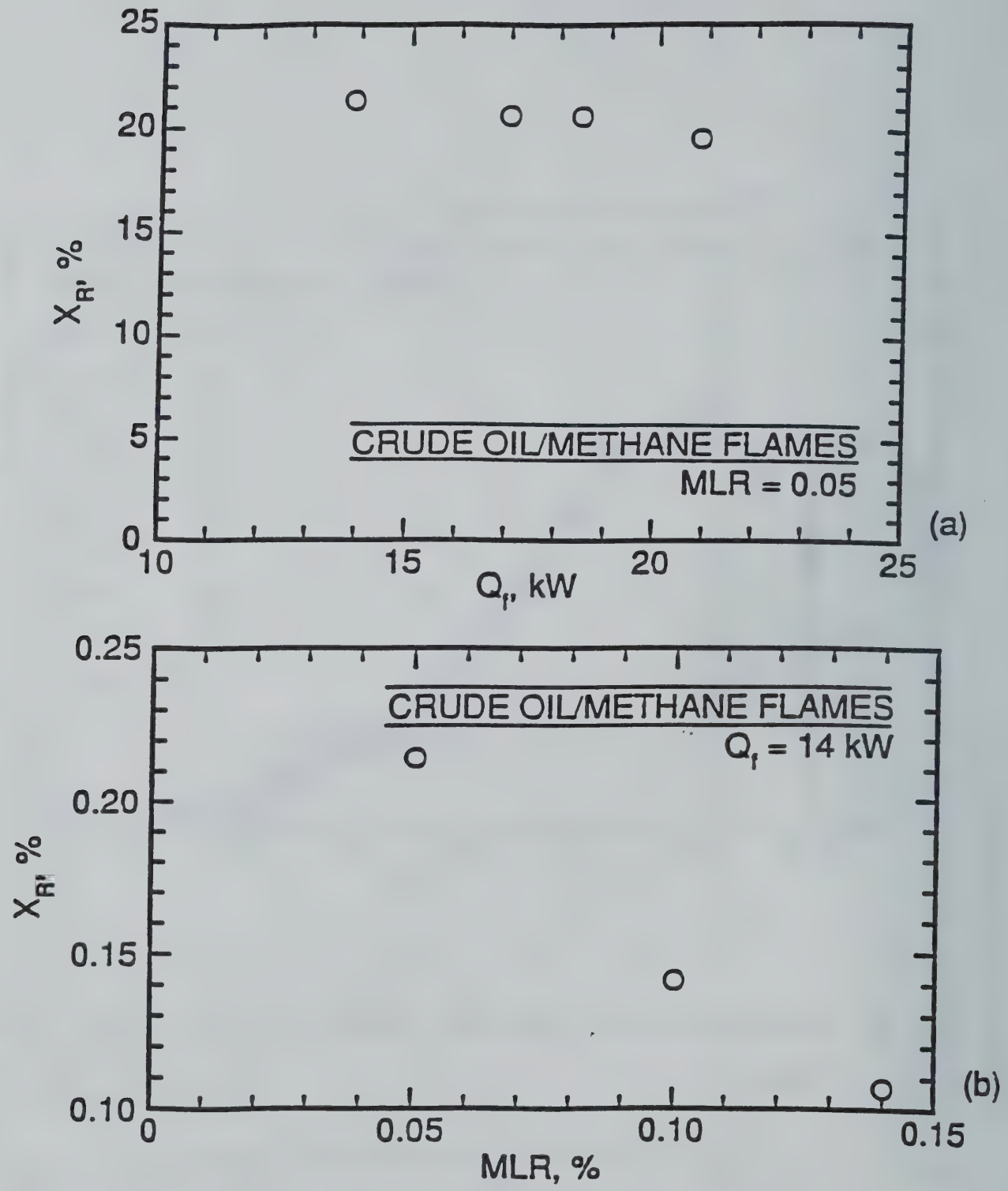

Fig. 7. Radiative heat loss fractions for crude-oil/methane flames as a function of heat release rate for a fixed methane-to-liquid ratio and as a function of methane-to-liquid ratio for a fixed heat release rate.

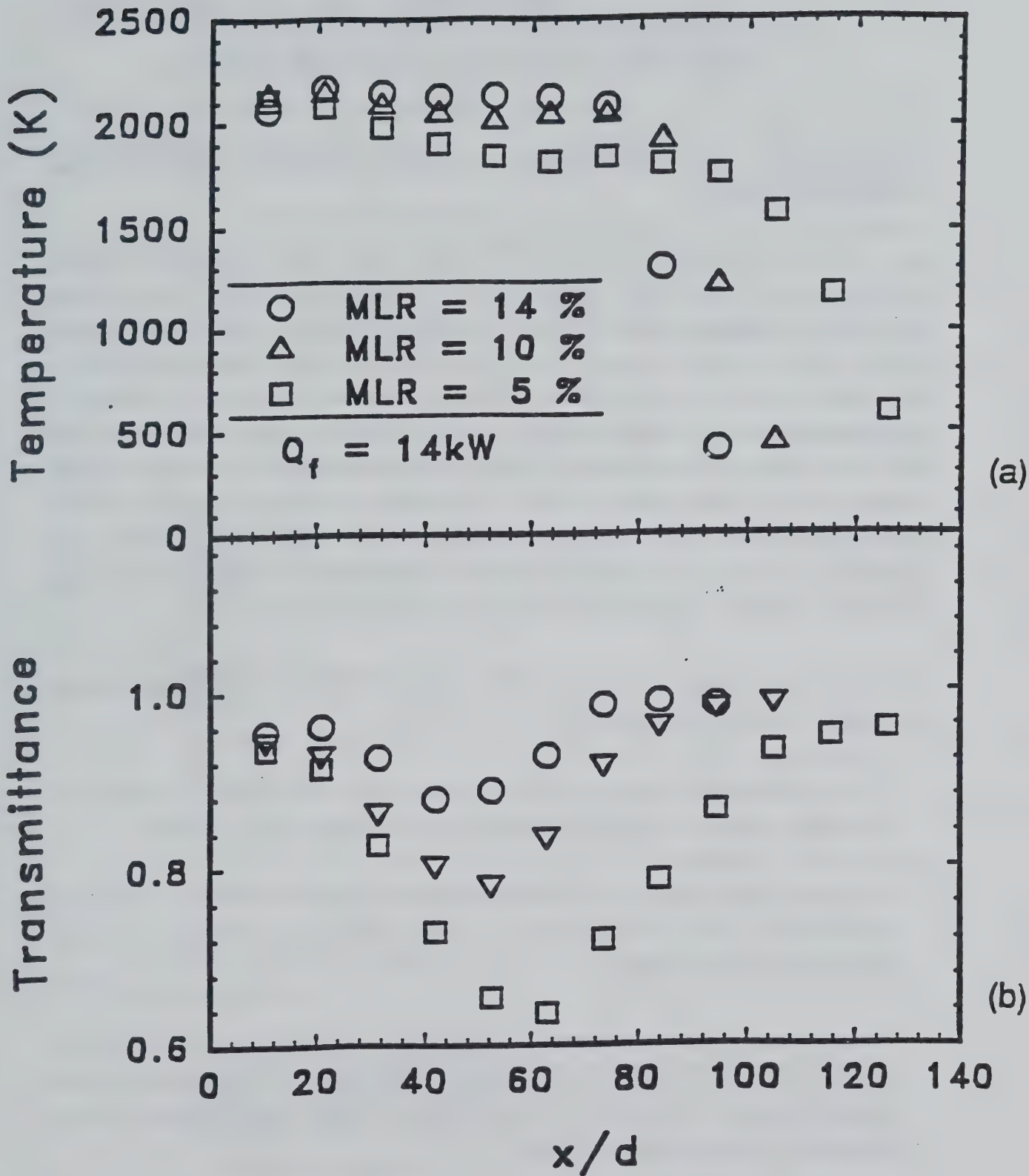

Fig. 8. Path integrated emission temperature measurements and soot transmittance measurements for crude-oil/methane spray flames with methane-to-liquid ratio as a parameter.

CHAPTER V

CONCLUSIONS AND RECOMMENDATIONS

SUMMARY OF IMPORTANT CONCLUSIONS FROM THE PRESENT GRANT

The objectives of the two-phase jet flame work during the current grant were: (1) to design an effervescent atomizer/burner for simulating high liquid loading jet flames; (2) to measure global properties (visible flame length, radiative heat flux to surrounding objects) of the flames stabilized on the burner; and (3) to complete path integrated measurements of emission temperature and monochromatic transmittance to help understand the behavior of the radiative flux. The present results for the visible flame height are also compared to those of Hustad and Sonju (Chapter IV) to highlight the effects of atomization quality on the flame length. The work required to meet these objectives has been completed. As described in the last three chapters, the major conclusions of this work are:

- Effervescent atomizer/burner can be used to stabilize high liquid loading flames in a jet configuration;

- The relationships between flame length and heat release rate or exit Reynolds number or Froude number show two phase flow effects;

- The single point heat flux measurement technique of Sivathanu and Gore (Chapter II) can be extended to spray flames to estimate the total radiative heat loss; and

- Work involving experiments at a larger scale and measurements of the two phase velocity distributions and evaporation characteristics in the spray flame are necessary for developing a basic understanding of the important processes in these fires.

RECOMMENDATIONS FOR FUTURE RESEARCH

Work completed during the present grant and a review of the literature has revealed several gaps in the present understanding of two-phase jet fires that need to be addressed.

(i) Two phase flow processes involving effects of drop size, heat of vaporization needed by the liquid and saturation of the drop environment by fuel vapor may lead to increase in flame height. These effects need to be understood qualitatively and quantitatively;

(ii) Separation between buoyant and forced flow regimes for scaling of two-phase flame heights is not currently understood;

(iii) Reduced entrainment rates due to higher jet density and possible variation in entrainment rates with fuel flow rate may also affect the flame length and need to be investigated;

(iv) Effects of low residence time due to high exit momentum on sooting tendency and radiative heat loss from high liquid loading jet flames need to be examined using fuels with high propensity for soot; and

(v) Scaling of the results from the 10-20 kW range to higher heat release rates needs to be examined.

These research objectives can be achieved by completing the following specific work:

(i) Measure Mie scattering from drops along the axis and along the radius at several locations in high liquid loading spray flames to determine the evaporation length and study its effects on the overall flame length;

(ii) Complete measurements of gas phase and liquid phase velocities using a phase discriminating Laser Doppler Velocimeter (LDV) as near the jet exit as possible to quantify the momentum flux for determining actual exit conditions for spray flames stabilized on the present burner;

(iii) Complete measurements of entrainment rates into spray jet flames using LDV to determine if changes in this process are causing the variations in the flame heights;

(iv) Complete measurements of flame heights, radiative loss fractions, temperature and path integrated transmitance for toluene spray flames atomized by ethylene to examine whether the residence times available in the spray flames suppress soot formation; and

(v) Construct and test an effervescent atomizer/burner for 100 to 200 kW heat release rate flames and measure flame heights and radiative fractions and attempt to obtain a two phase jet fire flame length correlation.

NIST-114
(REV. 6-93)
ADMAN 4.09

U.S. DEPARTMENT OF COMMERCE
NATIONAL INSTITUTE OF STANDARDS AND TECHNOLOGY

MANUSCRIPT REVIEW AND APPROVAL

(ERB USE ONLY)
ERB CONTROL NUMBER | DIVISION
PUBLICATION REPORT NUMBER: NIST-GCR-94-653 | CATEGORY CODE

INSTRUCTIONS: ATTACH ORIGINAL OF THIS FORM TO ONE (1) COPY OF MANUSCRIPT AND SEND TO THE SECRETARY, APPROPRIATE EDITORIAL REVIEW BOARD.

PUBLICATION DATE: June 1994 | NUMBER PRINTED PAGES

TITLE AND SUBTITLE (CITE IN FULL)
An investigatin of oil and gas well fires and flares

CONTRACT OR GRANT NUMBER
60NANB1D1172

TYPE OF REPORT AND/OR PERIOD COVERED
Final

AUTHOR(S) (LAST NAME, FIRST INITIAL, SECOND INITIAL)
P. Dutta, Y.R. Sivathanu, J.P. Gore
Purdue University
West Lafayette, IN

PERFORMING ORGANIZATION (CHECK (X) ONE BOX)
[ ] NIST/GAITHERSBURG
[ ] NIST/BOULDER
[ ] JILA/BOULDER

LABORATORY AND DIVISION NAMES (FIRST NIST AUTHOR ONLY)

SPONSORING ORGANIZATION NAME AND COMPLETE ADDRESS (STREET, CITY, STATE, ZIP)
US Department of Commerce
National Institute of Standarde and Technology
Gaithersburg, MD 20899

PROPOSED FOR NIST PUBLICATION

[ ] JOURNAL OF RESEARCH (NIST JRES)	[ ] MONOGRAPH (NIST MN)	[ ] LETTER CIRCULAR
[ ] J. PHYS. & CHEM. REF. DATA (JPCRD)	[ ] NATL. STD. REF. DATA SERIES (NIST NSRDS)	[ ] BUILDING SCIENCE SERIES
[ ] HANDBOOK (NIST HB)	[ ] FEDERAL INF. PROCESS. STDS. (NIST FIPS)	[ ] PRODUCT STANDARDS
[ ] SPECIAL PUBLICATION (NIST SP)	[ ] LIST OF PUBLICATIONS (NIST LP)	[X] OTHER NIST-GCR
[ ] TECHNICAL NOTE (NIST TN)	[ ] NIST INTERAGENCY/INTERNAL REPORT (NISTIR)	

PROPOSED FOR NON-NIST PUBLICATION (CITE FULLY) [ ] U.S. [ ] FOREIGN

PUBLISHING MEDIUM
[ ] PAPER [ ] CD-ROM
[ ] DISKETTE (SPECIFY)
[ ] OTHER (SPECIFY)

SUPPLEMENTARY NOTES

ABSTRACT (A 2000-CHARACTER OR LESS FACTUAL SUMMARY OF MOST SIGNIFICANT INFORMATION. IF DOCUMENT INCLUDES A SIGNIFICANT BIBLIOGRAPHY OR LITERATURE SURVEY, CITE IT HERE. SPELL OUT ACRONYMS ON FIRST REFERENCE.) (CONTINUE ON SEPARATE PAGE, IF NECESSARY.)

A theoretical and experimental study of jet flames with applications to large fires resulting from oil well and gas well accidents is reports. The results have been used in the interpretation of the single point radiation heat flux data collected around well fires in Kuwait. The significant accomplishments during the grant include: development of a technique to find total radiative heat loss from turbulent jet flames based on measurements of heat flux at a single location; design and successful operation of an effervescent atomizer/burner; study of global properties of the high liquid loading jet flames have shown that their lengths are affected by two-phase flow effects and that their soot loading and radiant output is lower than equivalent pool flames. The first time opportunity to study high liquid loading jet flames in the laboratory has led to a study with applications in the industrial safety and insurance-cost containment areas. Design of liquid handling and storage systems, areas around storage tanks and pipes, and fire safety and fire fighting procedures and effectiveness will benefit from the laboratory information concerning fire size, shape and radiant output.

KEY WORDS (MAXIMUM OF 9; 28 CHARACTERS AND SPACES EACH; SEPARATE WITH SEMICOLONS; ALPHABETIC ORDER; CAPITALIZE ONLY PROPER NAMES)
Fire research; oil wells fires; heat flux; jet flames; fire safety; pool fires; fire size

AVAILABILITY
[X] UNLIMITED [ ] FOR OFFICIAL DISTRIBUTION - DO NOT RELEASE TO NTIS
[ ] ORDER FROM SUPERINTENDENT OF DOCUMENTS, U.S. GPO, WASHINGTON, DC 20402
[X] ORDER FROM NTIS, SPRINGFIELD, VA 22161

NOTE TO AUTHOR(S): IF YOU DO NOT WISH THIS MANUSCRIPT ANNOUNCED BEFORE PUBLICATION, PLEASE CHECK HERE. [ ]